AFRL-IF-RS-TR-2001-186
Final Technical Report
September 2001

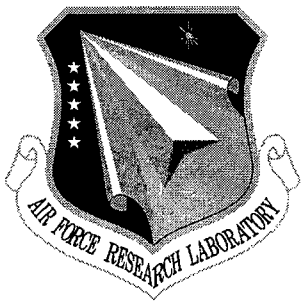

ANTI-JAMMING TECHNIQUES FOR GPS RECEIVERS

Villanova University

Moeness G. Amin, Alan R. Lindsey, Liang Zhao and Yimin Zhang

APPROVED FOR PUBLIC RELEASE; DISTRIBUTION UNLIMITED.

AIR FORCE RESEARCH LABORATORY
INFORMATION DIRECTORATE
ROME RESEARCH SITE
ROME, NEW YORK

20020117 027

This report has been reviewed by the Air Force Research Laboratory, Information Directorate, Public Affairs Office (IFOIPA) and is releasable to the National Technical Information Service (NTIS). At NTIS it will be releasable to the general public, including foreign nations.

AFRL-IF-RS-TR-2001-186 has been reviewed and is approved for publication.

APPROVED: ALAN R. LINDSEY
Project Engineer

FOR THE DIRECTOR: WARREN H. DEBANY, Jr.
Technical Advisor, Information Grid Division
Information Directorate

If your address has changed or if you wish to be removed from the Air Force Research Laboratory Rome Research Site mailing list, or if the addressee is no longer employed by your organization, please notify AFRL/IFGC, 525 Brooks Rd, Rome, NY 13441-4114. This will assist us in maintaining a current mailing list.

Do not return copies of this report unless contractual obligations or notices on a specific document require that it be returned.

REPORT DOCUMENTATION PAGE

Form Approved
OMB No. 0704-0188

Public reporting burden for this collection of information is estimated to average 1 hour per response, including the time for reviewing instructions, searching existing data sources, gathering and maintaining the data needed, and completing and reviewing the collection of information. Send comments regarding this burden estimate or any other aspect of this collection of information, including suggestions for reducing this burden, to Washington Headquarters Services, Directorate for Information Operations and Reports, 1215 Jefferson Davis Highway, Suite 1204, Arlington, VA 22202-4302, and to the Office of Management and Budget, Paperwork Reduction Project (0704-0188), Washington, DC 20503.

1. AGENCY USE ONLY *(Leave blank)*	2. REPORT DATE	3. REPORT TYPE AND DATES COVERED
	Sep 01	Final Apr 99 - Jan 01

4. TITLE AND SUBTITLE

ANTI-JAMMING TECHNIQUES FOR GPS RECEIVERS

5. FUNDING NUMBERS

C - F30602-99-2-0504
PE - 61102F
PR - 2304
TA - G9
WU - P2

6. AUTHOR(S)

Moeness G. Amin and Alan R. Lindsey

7. PERFORMING ORGANIZATION NAME(S) AND ADDRESS(ES)

Villanova University
800 Lancaster Ave
Villanova, PA 19085

8. PERFORMING ORGANIZATION REPORT NUMBER

9. SPONSORING/MONITORING AGENCY NAME(S) AND ADDRESS(ES)

AFRL/IFGC
525 Brooks Rd
Rome, NY 13441

10. SPONSORING/MONITORING AGENCY REPORT NUMBER

AFRL-IF-RS-TR-2001-186

11. SUPPLEMENTARY NOTES

AFRL Project Engineer: Alan R. Lindsey, IFGC, 315-330-1879

12a. DISTRIBUTION AVAILABILITY STATEMENT

Approved for public release; distribution unlimited.

12b. DISTRIBUTION CODE

13. ABSTRACT *(Maximum 200 words)*

The fundamental objective of this research project is to improve the GPS receiver performance when subjected to strong nonstationary interference. The techniques applied and proposed to achieve this objective rely on the estimation of both time-frequency and spatial signatures of the jammers. The report consists of four chapters addressing important problems in nonstationary interference mitigation in GPS receivers. The first two chapters deal with a single antenna receiver, whereas the last two chapters consider the presence of multi-antenna array. In all four chapters, the nonstationary interference is cast as an FM signal and it is mitigated using its temporal and spatial characteristics through subspace projection methods. The first three chapters are GPS specific and utilize the GPS signal structure and its deterministic nature. Chapter 4 applies to the general problem of suppressing instantaneous narrowband signals in broadband communication platforms.

14. SUBJECT TERMS

Interference Excision, spread-spectrum, time-frequency distribution, instantaneous frequency, nonstationary interference, jamming, jammer, signal conditioning, immune receivers, GPS, anti-jam, spatial processing, multi-sensor, multiple antenna, subspace projection

15. NUMBER OF PAGES

76

16. PRICE CODE

17. SECURITY CLASSIFICATION OF REPORT	18. SECURITY CLASSIFICATION OF THIS PAGE	19. SECURITY CLASSIFICATION OF ABSTRACT	20. LIMITATION OF ABSTRACT
UNCLASSIFIED	UNCLASSIFIED	UNCLASSIFIED	UL

Standard Form 298 (Rev. 2-89) (EG)
Prescribed by ANSI Std. 239.18
Designed using Perform Pro, WHS/DIOR, Oct 94

Anti-Jamming Techniques for GPS Receivers

Executive Summary

This is the final report for the Air Force Research Lab (AFRL) contract no. F30602-99-2-0504. It provides research results obtained over the period of April 1999 to January 2001.

The contributors to the research over the span of the contract are Professor Moeness Amin (PI), Dr. Yimin Zhang (Postdoctoral Fellow), and Mr. Liang Zhao (Graduate Student) from Villanova University. Dr. Alan Lindsey (Project Manager) from AFRL has worked closely with the research team at Villanova University and has provided valuable insights into several issues vital to progress and advances in research. Both Dr. Zhang and Mr. Zhao continue to work on GPS signal processing for ant-jamming. They, along with Prof. Amin, are supported by a new contract from the AFRL.

The fundamental objective of this research project is to improve the GPS receiver performance when subjected to strong nonstationary interference. The techniques applied and proposed to achieve this objective rely on the estimation of both time-frequency and spatial signatures of the jammers.

The report consists of four chapters addressing important problems in nonstationary interference mitigation in GPS receivers. Each chapter has its own abstract, introduction, equation numbers, figure numbers and captions, appendices, conclusions, and references. The first two chapters deal with a single antenna receiver, whereas the last two chapters consider the presence of multi-antenna array. In all four chapters, the nonstationary interference is cast as an FM signal and it is mitigated using its temporal and spatial characteristics through subspace projection methods. The first three chapters are GPS specific and utilize the GPS signal structure and its deterministic nature. Chapter 4 applies to the general problem of suppressing instantaneous narrowband signals in broadband communication platforms.

Subspace projection techniques are applied in Chapter 1 as a pre-correlation signal processing method for FM interference suppressions in GPS receivers. The FM jammers are instantaneous narrowband and have clear time-frequency (t-f) signatures that are distinct from the GPS C/A spread spectrum code. In the proposed technique, the instantaneous frequency (IF) of the jammer is estimated and used to construct a rotated signal space in which the jammer occupies one dimension. The anti-jamming system is implemented by projecting the received data sequence onto the jammer-free subspace. Chapter 1 focuses on the characteristics of the GPS C/A code and derives the signal to interference and noise ratio (SINR) of the GPS receiver, implementing the subspace projection techniques.

Frequency modulated signals in the frequency band 1.217-1.238 GHz and 1.565-1.586 GHz present a source of interference to the GPS, which should be properly

mitigated. The problem of mitigating periodic interferers in GPS receivers using subspace projection techniques is addressed in chapter 2. In this Chapter, the signal-to-interference-and-noise ratio (SINR) of the GPS receiver implementing subspace projection techniques for suppression of FM jammers is derived. The general case in which the jammer may have equal or different cycles than the coarse acquisition (C/A) code of the GPS signals is considered. It is shown that the weak correlations between the FM interference and the gold codes allow effective interference cancellation without significant loss of the desired signal

Subspace array processing for the suppression of FM jammers in GPS receivers is introduced in Chapter 3. In this Chapter, subspace projection array processing techniques are applied for suppression of frequency modulated (FM) jammers in GPS receivers. In the proposed technique, the instantaneous frequency (IF) of the jammer is estimated and used to construct the jammer subspace. With a multi-sensor receiver, both spatial and time-frequency signatures of signal arrivals are used for effective interference suppression. Chapter 3 considers the deterministic nature of the GPS C/A code. The receiver SINR is derived and shown to offer improved performance in strong interference environments.

Combined spatial and time-frequency signatures of signal arrivals at a multi-sensor array are used in Chapter 4 for nonstationary interference suppression in direct-sequence spread-spectrum (DS/SS) communications. With random PN spreading code and deterministic nonstationary interferers, the use of antenna arrays offers increased DS/SS signal dimensionality relative to the interferers. Interference mitigation through spatio-temporal subspace projection technique leads to reduced DS/SS signal distortion and improved performance over the case of a single antenna receiver. The angular separation between the interference and desired signals is shown to play a fundamental role in trading off the contribution of the spatial and time-frequency signatures to the interference mitigation process. The expressions of the receiver SINR implementing subspace projections are derived and numerical results are provided.

Following this executive summary are the lists of papers submitted/published based on the above contributions. The four chapters included in this report properly integrate and extensively cover the material presented in all paper submissions under this contract.

List of Journal Publications

[1] Yimin Zhang, and M. G. Amin, "Array Processing for Nonstationary Interference Suppression in DS/SS Communications Using Subspace Projection Techniques," submitted to *IEEE Trans. Signal Processing*, Sept. 2000. Revised March 2001.

List of Conference Publications

[1] L. Zhao, M. G. Amin, and A. R. Lindsey, "Subspace projection techniques for anti-FM jamming GPS receivers," *Proceedings of the 10-th IEEE Workshop on Statistical Signal and Array Processing*, pp. 529-533, Aug. 2000.

[2] L. Zhao, M. G. Amin, and A. R. Lindsey, "Subspace Array Processing for the Suppression of FM Jamming in GPS Receivers," *Proceedings of the Asilomar Conference on Signals, Systems, and Computers*, Monterey, CA, Oct. 2000.

[3] L. Zhao, M. G. Amin, and A. R. Lindsey, "Mitigation of Periodic Interferers in GPS Receivers Using Subspace Projection Techniques," Submitted to *ICASSP 2001*, Dec. 2000.

List of Conference Presentations

[1] L. Zhao, M. G. Amin, and A. R. Lindsey, "Subspace projection techniques for anti-FM jamming GPS receivers," *the 10-th IEEE Workshop on Statistical Signal and Array Processing*, pp. 529-533, Aug. 2000. Presented by L. Zhao.

[2] L. Zhao, M. G. Amin, and A. R. Lindsey, "Subspace Array Processing for the Suppression of FM Jamming in GPS Receivers," *the Asilomar Conference on Signals, Systems, and Computers*, Monterey, CA, Oct. 2000. Presented by A. R. Lindsey.

Chapter 1

Subspace Projection Techniques for Anti-FM Jamming GPS Receivers

Abstract

This report applies subspace projection techniques as a pre-correlation signal processing method for the FM interference suppressions in GPS receivers. The FM jammers are instantaneous narrowband and have clear time-frequency (t-f) signatures that are distinct from the GPS C/A spread spectrum code. In the proposed technique, the instantaneous frequency (IF) of the jammer is estimated and used to construct a rotated signal space in which the jammer occupies one dimension. The anti-jamming system is implemented by projecting the received sequence onto the jammer-free subspace. This report focuses on the characteristics of the GPS C/A code and derives the signal to interference and noise ratio (SINR) of the GPS receivers implementing the subspace projection techniques.

I. Introduction

The Global Positioning System (GPS) is a satellite-based, worldwide, all-weather navigation and timing system [1]. The ever-increasing reliance on GPS for navigation and guidance has created a growing awareness of the need for adequate protection against both unintentional and intentional interference. Jamming is a procedure that attempts to block reception of the desired signal by the intended receiver. In general terms, it is high power signal that occupies the same frequency as the desired signal, making reception by the intended receiver difficult or impossible. Designers of military as well as commercial communication systems have, through the years, developed numerous anti-jamming techniques to counter these threats. As these techniques become effective for interference removal and mitigation, jammers themselves have become smarter and more sophisticated, and generate signals, which are difficult to combat.

The GPS system employs BPSK-modulated direct sequence spread spectrum (DSSS) signals. The DSSS systems are implicitly able to provide a certain degree of protection against intentional or non-intentional jammers. However, in many cases, the jammer may be much stronger than the GPS signal, and the spreading gain might be insufficient to decode the useful data reliably [2]. There are several methods that have been proposed for interference suppression in DSSS communications [3], [4], [5]. The recent development of the bilinear time-frequency distributions (TFDs) for improved signal power localization in the time-frequency plane has motivated several new effective approaches, based on instantaneous frequency (IF) estimation, for non-stationary interference excisions [6]. One of the important IF-based interference rejection techniques uses the jammer IF to construct a time-varying excision notch filter that effectively removes the interference [7]. However, this notch filtering excision technique causes significant distortions to the desired signal, leading to undesired receiver performance.

Recently, subspace projection techniques, which are also based on IF estimation, have been devised for non-stationary FM interference excision in DSSS communications [8]. The techniques assume clear jammer time-frequency signatures and rely on the distinct differences in the localization properties between the jammer and the spread spectrum signals. The jammer instantaneous frequency, whether provided by the time-frequency distributions or any other IF estimator, is used to form an interference subspace. Projection can then be performed to excise the jammer from the incoming signal prior to correlation with the receiver PN sequence. The result is improved receiver SINR and reduced BERs.

In this report, we apply the subspace projection techniques as a pre-correlation signal processing method to the FM interference suppression in GPS receivers. The GPS receiver and signal structure impose new constraints on the problem since the spreading code from each satellite is known and periodic within one navigation data symbol. This structure and the signal model are reviewed in Section 2. In Section 3, we depict the received GPS signal properties in time-frequency domain. The SINR of the GPS receiver implementing the subspace projection techniques is derived in Section 4, which shows improved performance in strong interference environments.

II. Signal Model

GPS employs BPSK-modulated DSSS signals. The navigation data is transmitted at a symbol rate of 50 bps. It is spread by a coarse acquisition (C/A) code and a precision (P) code. The C/A code is a Gold sequence with a chip rate of 1.023 MHz and a period of 1023 chips, i.e. its period is 1ms, and there are 20 periods within one data symbol. The P code is a pseudorandom code at the rate of 10.23 MHz and with a period of 1 week. These two spreading codes are multiplexed in quadrature phases. Figure 1 shows the signal structure. The carrier L1 is modulated by both C/A code and P code, whereas the carrier L2 is only modulated by P code. In this report, we will mainly address the problem of anti-jamming

for the C/A code, for which the peak power spectral density exceeds that of the P code by about 13 dB [1]. The transmitted GPS signal is also very weak with Jammer-to-Signal Ratio (JSR) often larger than 40 dB and Signal-to-Noise Ratio (SNR) in the range -14 to -20 dB [2], [9]. Due to the high JSR, the FM jammer often has a clear signature in the time-frequency domain as shown in Section 3. As the P code is very weak compared to the C/A code, noise and jammer, we can ignore its presence in our analysis.

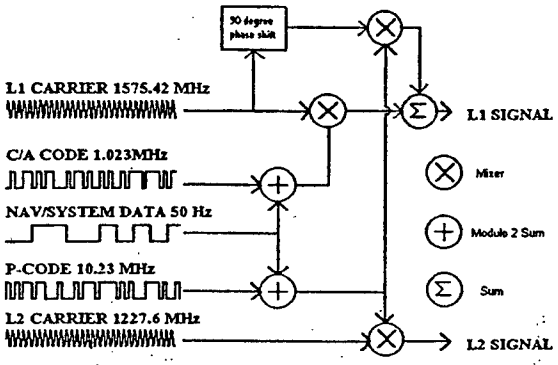

Fig. 1. The GPS signal structure.

The BPSK-modulated DSSS signal may be expressed as

$$s(t) = \sum_i I_i \; b_i(t - iT_b) \qquad I_i \in \{-1, 1\} \forall i \tag{1}$$

where I_i represents the binary information sequence and T_b is the bit interval, which is 20ms in the case of GPS system. The i^{th} binary information bit, $b_i(t)$ is further decomposed as a superposition of L spreading codes, $p(n)$, pulse shaped by a unit-energy function, $q(t)$, of duration of τ_c, which is 1/1023 ms in the case of C/A code. Accordingly,

$$b_i(t) = \sum_{n=1}^{L} p(n) \; q(t - n\tau_c) \tag{2}$$

The signal for one data bit at the receiver, after demodulation, and sampling at chip rate, becomes

$$x(n) = p(n) + w(n) + j(n) \qquad 1 \leq n \leq L \tag{3}$$

where $p(n)$ is the chip sequence, $w(n)$ is the white noise, and $j(n)$ is the interfering signal. The above equation can be written in the vector form

$$\mathbf{x} = \mathbf{p} + \mathbf{w} + \mathbf{j} \tag{4}$$

where

$$\begin{aligned}
\mathbf{x} &= \begin{bmatrix} x(1) & x(2) & x(3) & \cdots & x(L) \end{bmatrix}^T, \\
\mathbf{p} &= \begin{bmatrix} p(1) & p(2) & p(3) & \cdots & p(L) \end{bmatrix}^T \\
\mathbf{w} &= \begin{bmatrix} w(1) & w(2) & w(3) & \cdots & w(L) \end{bmatrix}^T, \\
\mathbf{j} &= \begin{bmatrix} j(1) & j(2) & j(3) & \cdots & j(L) \end{bmatrix}^T
\end{aligned}$$

All vectors are of dimension $L \times 1$, and 'T' denotes vector or matrix transposition. It should be noted that the P vector is real, whereas all other vectors in the above equation have complex enteries.

III. Periodic Signal Plus Jammer in the Time-Frequency Domain

For GPS C/A code, the PN sequence is periodic. The PN code of length 1023 repeats itself 20 times within one symbol of the 50 bps navigation data. Consequently, it is no longer of a continuous spectrum in the frequency domain, but rather of spectral lines. The case is the same for periodic jammers. Figure 2 and Figure 3 show the effect of periodicity of the signal and the jammer on their respective power distribution over time and frequency, using Wigner-Ville distribution. In both figures, a PN sequence of length 32 samples that repeats 8 times is used. A non-periodic chirp jammer of a 50dB JSR (jammer-to-signal ratio) is added in Figure 2. A periodic chirp jammer of 50 dB JSR with the same period as the C/A code is included in Figure 3. We note that the chosen value of 50dB JSR has a practical significance. The spread spectrum systems in a typical GPS C/A code receiver can tolerate a narrowband interference of approximately 40 dB

JSR without interference mitigation processing. However, field tests show that jammer strength often exceeds that number due to the weakness of the signal. SNR in both figures are -20dB, which is also close to its practical value [2], [9]. Due to high JSR, the jammer is dominant in both figures. From Figure 3, it is clear that the periodicity of the jammer brings more difficulty to IF estimation than the non-periodic jammers. This problem can be solved by applying a short data window when using Wigner-Ville distribution. Note that the window length should be less than the jammer period. Figure 4 shows the result of applying a window of length 31 to the same data used in Fig. 3. It is evident from the Fig. 4 that the horizontal discrete harmonic lines have disappeared.

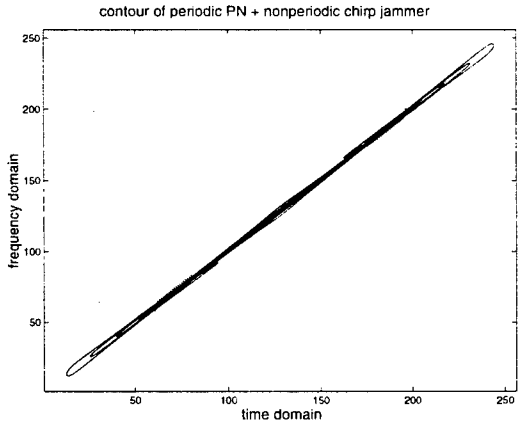

Fig. 2. Periodic signal corrupted by a non-periodic jammer in time-frequency domain

IV. GPS Anti-Jamming Using Projection Techniques

The concept of subspace projection for instantaneously narrowband jammer suppression is to remove the jammer components from the received data by projecting it onto the subspace that is orthogonal to the jammer subspace, as illustrated in Fig. 5.

Once the instantaneous frequency (IF) of the non-stationary jammer is estimated from the time-frequency domain, or by using any other IF estimator [10], [11], [12], [13], the interference signal vector $\mathbf{j}$ in (4) can be constructed, up to ambiguity in phase and possibly

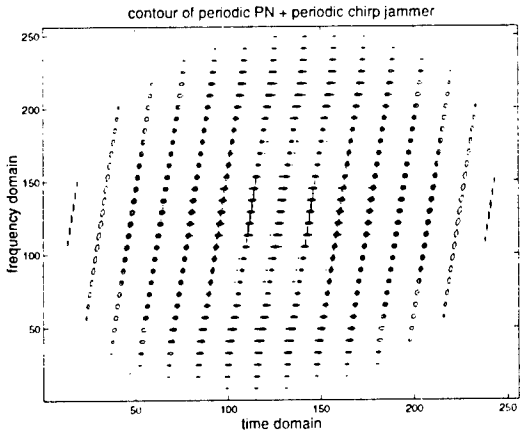

Fig. 3. Periodic signal corrupted by a periodic jammer in time-frequency domain

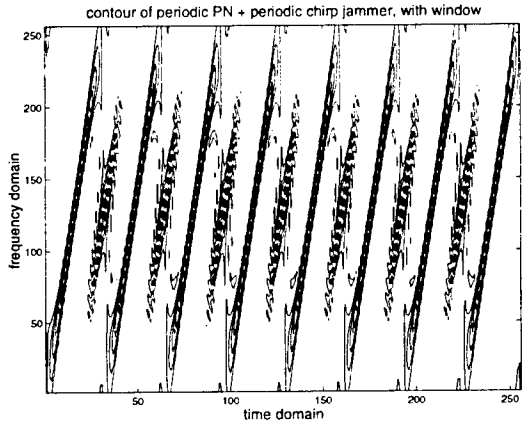

Fig. 4. Periodic signal corrupted by a periodic jammer in time-frequency domain (with window)

in amplitude. In the proposed interference excision approach, the data vector is partitioned into Q blocks, each of length P, i.e. L=PQ. For the GPS C/A code, Q=20, P=1023, and all Q blocks are identical, i.e., the signal PN sequence is periodic. Block-processing provides the flexibility to discard the portions of the data bit, over which there are significant errors in the IF estimates. The orthogonal projection method makes use of the fact that, in each block, the jammer has a one-dimensional subspace $\mathcal{J}$ in the P-dimensional space $\mathcal{V}$, which is spanned by the received data vector. The interference can be removed from each block by projecting the received data on the corresponding orthogonal subspace $\mathcal{G}$ of

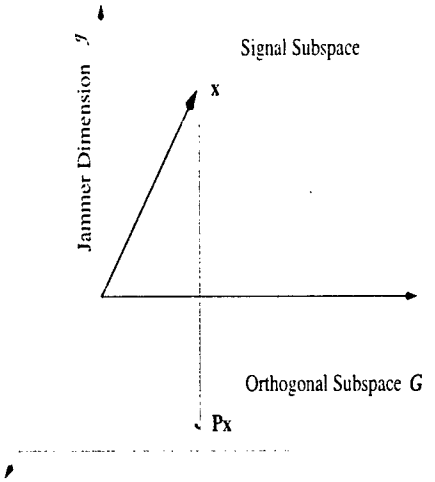

Fig. 5. Jammer excision by subspace projection

interference subspace $\mathcal{J}$. The subspace $\mathcal{J}$ is estimated using the IF information. The projection matrix for the k^{th} block is given by

$$\mathbf{V}_k = \mathbf{I} - \mathbf{u}_k \ \mathbf{u}_k^H \tag{5}$$

The vector $\mathbf{u}_k$ is the unit norm basis vector in the direction of the interference vector of the k^{th} block, and 'H' denotes vector or matrix Hermitian. Since the FM jammer signals are uniquely characterized by their IFs, the i^{th} FM jammer in the k^{th} block can be expressed as

$$u_k(i) = \frac{1}{\sqrt{P}} exp[j\phi_k(i)] \tag{6}$$

The result of the projection over the k^{th} data block is

$$\bar{\mathbf{x}}_k = \mathbf{V}_k \ \mathbf{x}_k \tag{7}$$

where $\mathbf{x}_k$ is the input data vector. Using the three different components that make up the input vector in (4), the output of the projection filter $\mathbf{V}_k$ can be written as

$$\bar{\mathbf{x}}_k = \mathbf{V}_k \ [\mathbf{p}_k + \mathbf{w}_k + \mathbf{j}_k] \tag{8}$$

The noise is assumed to be complex white Gaussian with zero-mean,

$$E[w(n)] = 0, \ E[w(n)^* w(n+l)] = \sigma^2 \delta(l), \forall l \tag{9}$$

Since we assume total interference excision through the projection operation, then

$$\mathbf{V}_k \mathbf{j}_k = 0, \qquad \bar{\mathbf{x}}_k = \mathbf{V}_k \, \mathbf{p}_k + \mathbf{V}_k \, \mathbf{w}_k \tag{10}$$

The decision variable y_r is the real part of y that is obtained by correlating the filter output $\bar{\mathbf{x}}_k$ with the corresponding kth block of the receiver PN sequence and summing the results over the K blocks. That is,

$$y = \sum_{k=0}^{K-1} \bar{\mathbf{x}}_k^H \, \mathbf{p}_k \tag{11}$$

Since the PN code is periodic, we can strip off the subscript k in p_k. The above variable can be written in terms of the constituent signals as

$$y = \sum_{k=0}^{Q-1} \mathbf{p}^T \mathbf{V}_k \mathbf{p} + \sum_{k=0}^{Q-1} \mathbf{w}^H \mathbf{V}_k \mathbf{p} \triangleq y_1 + y_2 \tag{12}$$

where y_1 and y_2 are the contributions of the PN and noise sequences to the decision variable, respectively. In [8], y_1 is considered as a random variable. However, in GPS system, due to the fact that each satellite is assigned a fixed Gold code [1], and that the Gold code is the same for every navigation data symbol, y_1 can no longer be treated as a random variable, but rather a deterministic value. This is a key difference between the GPS system and other spread spectrum systems. The value of y_1 is given by

$$\begin{aligned} y_1 &= \sum_{k=0}^{Q-1} \mathbf{p}^T \mathbf{V}_k \mathbf{p} \\ &= \sum_{k=0}^{Q-1} \mathbf{p}^T (\mathbf{I} - \mathbf{u}_k \mathbf{u}_k^H) \mathbf{p} \\ &= \sum_{k=0}^{Q-1} (\mathbf{p}^T \mathbf{p} - \mathbf{p}^T \mathbf{u}_k \mathbf{u}_k^H \mathbf{p}) \\ &= QP - \sum_{k=0}^{Q-1} (\mathbf{p}^T \mathbf{u}_k \mathbf{u}_k^H \mathbf{p}) \end{aligned} \tag{13}$$

Define

$$\beta_k = \frac{\mathbf{p}^T \mathbf{u}_k}{\sqrt{P}} \tag{14}$$

as the correlation coefficient between the PN sequence vector $\mathbf{p}$ and the jammer vector $\mathbf{u}$. β_k reflects the the component of the signal that is in the jammer subspace, and represents the degree of resemblance between the signal sequence and the jammer sequence. Since the signal is a PN sequence, and the jammer is a non-stationary FM signal, the correlation coefficient is typically very small. With the above definition, y_1 can be expressed as

$$y_1 = P(Q - \sum_{k=0}^{Q-1} |\beta_k|^2) \tag{15}$$

From (15), it is clear that y_1 is a real value, which is the result of the fact that the projection matrix V is Hermitian. With the assumptions in (9), y_2 is complex white Gaussian with zero-mean. Therefore,

$$\begin{aligned}
\sigma_{y_2}^2 &= E\left[|y_2|^2\right] \\
&= E\left[(\sum_{k=0}^{Q-1} \mathbf{w}^H \mathbf{V}_k \mathbf{p})^H (\sum_{l=0}^{Q-1} \mathbf{w}^H \mathbf{V}_l \mathbf{p})\right] \\
&= \sum_{k=0}^{Q-1}\sum_{l=0}^{Q-1} \mathbf{p}^T \mathbf{V}_k E\left[\mathbf{w}_k \mathbf{w}_l^H\right] \mathbf{V}_l \mathbf{p} \\
&= \sum_{k=0}^{Q-1} \mathbf{p}^T \mathbf{V}_k E\left[\mathbf{w}_k \mathbf{w}_k^H\right] \mathbf{V}_k \mathbf{p} \\
&= \sigma^2 \sum_{k=0}^{Q-1} \mathbf{p}^T \mathbf{V}_k \mathbf{V}_k \mathbf{p} \\
&= \sigma^2 \sum_{k=0}^{Q-1} \mathbf{p}^T \mathbf{V}_k \mathbf{p} = \sigma^2 y_1
\end{aligned} \tag{16}$$

the above equations make use of the noise assumptions in (9) and the properties of the projection matrix. The decision variable y_r is the real part of y. Consequently, y_r is given by

$$y_r = y_1 + Re\{y_2\} \tag{17}$$

where $Re\{y_2\}$ denotes the real part of y_2. $Re\{y_2\}$ is real white Gaussian with zero-mean and variance $\frac{1}{2}\sigma_{y_2}^2$. Therefore, the SINR is

$$SINR = \frac{y_1^2}{var\{Re\{y_2\}\}}$$

$$= \frac{y_1^2}{\frac{1}{2}\sigma_{y_2}^2} = \frac{2y_1}{\sigma^2}$$
$$= \frac{2P(Q - \sum_{k=0}^{Q-1} |\beta_k|^2)}{\sigma^2} \quad (18)$$

In the absence of jammers, no excision is necessary, and the SINR(SNR) of the receiver output will become $2PQ/\sigma^2$, which represents the upper bound for the anti-jamming performance. Clearly, $\frac{2P\sum_{k=0}^{Q-1}|\beta_k|^2}{\sigma^2}$ is the reduction in the receiver performance caused by the proposed jammer suppression techniques. It reflects the energy of the power of the signal component that is in the jammer subspace. If the jammer and spread spectrum signals are orthogonal, i.e., their correlation coefficient $|\beta| = 0$, then interference suppression is achieved with no loss in performance. However, as stated above, in the general case, β_k is often very small, so the projection technique can excise FM jammers effectively with only very insignificant signal loss. The lower bound of SINR is zero and corresponds to $|\beta| = 1$. This case requires the jammer to assume the C/A code, i.e., identical and synchronous with actual one. Figure 6 depicts the theoretical SINR in (18), its upper bound, and estimated values using computer simulation. The SNR assumes five different values [-25, -20, -15, -10,-5] dB. In this figure, the signal is the Gold code of satellite SV#1, and the jammer is a periodic chirp FM signal with frequency 0–0.5 and has the same period as the C/A code. For this case, the correlation coefficient β is very small, $|\beta| = 0.0387$. JSR used in the computer simulation is set to 50dB. Due to the large computation involved, we have used 1000 realizations for each SNR value. Figure 6 demonstrates that the theoretical value of SINRs is almost the same as the upper bound and both are very close to the simulation result. In the simulation as well as in the derivation of equation (18), we have assumed exact knowledge of the jammer IF. Inaccuracies in the IF estimation will have an effect on the receiver performance [8].

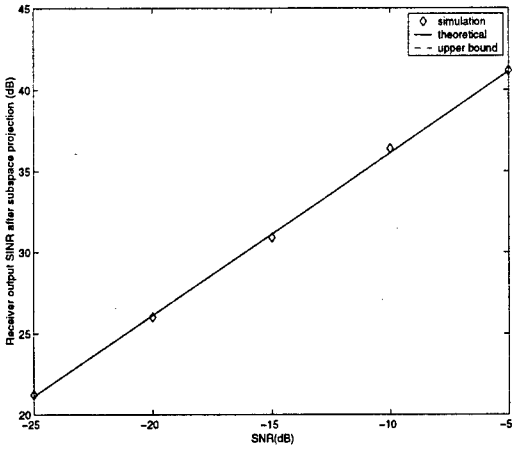

Fig. 6. Receiver SINR vs SNR.

V. Conclusions

GPS receivers are vulnerable to strong interferences. In this report, subspace projection techniques are adapted for the anti-FM jamming GPS receiver. These techniques are based on IF estimation of the jammer signal, which can be easily achieved, providing that the C/A code and the jammer have distinct time-frequency signatures. The IF information is used to construct the FM interference subspace which, because of signal nonstationarities, is otherwise difficult to obtain. Due to the characteristic of the GPS spread spectrum signal structure and the fact that the C/A codes are fixed for the different satellites and known to all, the analysis of the receiver SINR becomes different from common spread spectrum systems. The theoretical and simulation results suggest that the subspace projection techniques can effectively excise FM jammers for GPS receivers with insignificant loss in the spreading gain.

References

[1] B. W. Parkinson and J. J. Spilker Jr. eds, *Global Positioning System: Theory and Applications*, American Institute of Aeronautics and Astronautics, 1996.

[2] M. S. Braasch and A. J. Van Dierendonck, "GPS receiver architectures and measurements," *Proceedings of the IEEE*, vol. 87, no. 1, pp. 48–64, Jan. 1999.

[3] L. B. Milstein, "Interference rejection techniques in spread spectrum communications," *Proceedings of the IEEE*, vol. 76, no. 6, pp. 657–671, Jun. 1988.

[4] H. V. Poor and L. A. Rusch, "Narrowband interference suppression in spread spectrum CDMA," *IEEE Personal Communications Magazine*, third quarter, pp. 14-27, 1994.

[5] J. D. Laster and J. H. Reed, "Interference rejection in digital wireless communications," *IEEE Signal Processing Magazine*, pp. 37-62, May 1997.

[6] M. G. Amin and A. N. Akansu, "Time-frequency for interference excision in spread-spectrum communications," in "Highlights of Signal Processing for Communications," *IEEE Signal Processing Magazine*, vol. 16, no. 2, pp. 33–34, March 1999.

[7] M.G. Amin, C. Wang and A. Lindsey, "Optimum interference excision in spread spectrum communications using open loop adaptive filters," *IEEE Trans. on Signal Processing*, vol. 47, no. 7, pp. 1966-1976, July 1999.

[8] M.G. Amin, R. S. Ramineni and A. Lindsey, "Interference excision in DSSS communication systems using projection techniques," submitted to *IEEE Trans. on Signal Processing*, Jan. 2000.

[9] R. Jr. Landry, P. Mouyon and D. Lekaim, "Interference mitigation in spread spectrum systems by wavelet coefficients thresholding," *European Trans. on Telecommunications*, vol. 9, pp. 191-202 March-Apr. 2000.

[10] B. Boashash, "Estimating and interpreting the instantaneous frequency of a signal," Parts 1 and 2, *Proceedings of the IEEE*, vol. 80, no. 12, Dec. 1990.

[11] S. Kay, "A fast and accurate single frequency estimator," *IEEE Trans. on Acoustics, Speech, and Signal Processing*, vol. 37, no. 12, Dec. 1979.

[12] L. Cohen, *Time-Frequency Analysis* , Prentice Hall, Englewood Cliffs, New Jersey, 1995.

[13] L. White. "Adaptive tracking of frequency modulated signals using hidden markov models." *Workshop on Hidden Markov Models For Tracking. Wirrina Cove Resort*, Feb. 1992.

Chapter 2

Mitigation of Periodic Interferers in GPS Receivers Using Subspace Projection Techniques

Abstract

Frequency modulated signals in the frequency band 1.217-1.238 GHz and 1.565-1.586 GHz present a source of interference to the GPS, which should be properly mitigated. In this report, we derive the Signal-to-Interference-and-Noise Ratio (SINR) of the GPS receiver implementing subspace projection techniques for suppression of FM jammers. We consider the general case in which the jammer may have equal or different cycles than the coarse acquisition (C/A) code of the GPS signals. It is shown that the weak correlations between the FM interference and the Gold codes allow effective interference cancellation without significant loss of the desired signal

I. Introduction

Subspace projection techniques based on time-frequency distributions have been employed for suppression of non-stationary FM interference in broadband communication platforms [1]-[4]. Most recently, they have been applied to Global Positioning System (GPS) with single [5] and multi-sensor [6] receivers. These techniques assume clear jammer time-frequency signatures and rely on the distinct differences in the localization properties between the interference FM waveforms and the coarse acquisition (C/A) Gold codes of the GPS signals. The FM jammer instantaneous frequency (IF), whether provided by the time-frequency distributions or any other IF estimator [7][8], is used to define the temporal signature of the interference, which is in turn used to construct the interference subspace. The respective projection matrix is used to excise the jammer power in the incoming signal prior to correlation with the receiver C/A codes. The result is improved receiver signal-to-interference-plus-noise ratio (SINR) and reduced BERs.

In this report, we generalize the results in Chapter 1 and reference [5] by considering jammer signals with different periodic structures from that of the GPS C/A codes. In the underlying problem, we deal with the case in which multiplicities of the jammer period span a finite number of the GPS information symbols. Therefore, unlike the previous work that assumes periodic synchronization between the interference and the desired signal, the generalization herein allows different portions of the jammer signal to infringe on different symbols of the GPS C/A code. It is shown, however, that due to the weak correlation between the FM waveforms and the Gold codes, the GPS receiver

implementing subspace projections is robust to FM jammer periodic patterns and repetition cycles, achieving full interference suppression with no significant performance degradation from that obtained in the optimum interference free environment.

II. SINR Analysis for Periodic Jammers

The derivation in Chapter 1 implicitly assumes that the jammer period, T_j, is equal to the symbol length, T_g, of the GPS signal, i.e., $T_j=T_g=PQ$. This assumption limits the *SINR* result

$$SINR = 2P\left(Q - \sum_{k=0}^{Q-1}|\beta_k|^2\right)\Big/\sigma^2 \tag{1}$$

to the special case where the jammer and GPS signals have the same cycle. Considering the more general case, the jammer is presumed to be a periodic signal with $T_j = \frac{N}{M}PQ$, where N and M are integers and relatively prime. Recall that P=1023 is the period of the GPS spreading code, and Q=20 is the number of times the code repeats itself over one symbol. From the above definition, M jammer periods extend over N symbols of the GPS signal, and, as such, different segments of the jammer signature will infringe on different GPS symbols. Therefore, in the analysis herein, we add the subscript i to associate the receiver variables with the k^{th} symbol. It is straightforward to show that the correlation output at the receiver yields

$$y_i = \sum_{k=0}^{Q-1}\mathbf{p}^T\mathbf{V}_{ik}\mathbf{p} + \sum_{k=0}^{Q-1}\mathbf{w}^T(n)\mathbf{V}_{ik}\mathbf{p}\underline{\Delta}y_{i1} + y_{i2} \tag{2}$$

The decision variable is the real part of y_i. It can be shown that

$$y_{i1} = P(Q - \sum_{k=0}^{Q-1}|\beta_{ik}|^2) \tag{3}$$

On the other hand, the correlation output due to the noise, y_{i2}, is a complex Gaussian zero-mean random variable, and its variance can be readily obtained as

$$\sigma_{y_{i2}}^2 = \sigma^2 P(Q - \sum_{k=0}^{Q-1} |\beta_{ik}|^2) \tag{4}$$

It is noted that since there are N symbols for every M jammer periods, and $M \neq N$, both variables y_{i1} and y_{i2} assume different values over N consecutive GPS symbols. The jammer can then be cast as symbol-dependent, assuming N distinct waveforms. In this case, one simple measure of the receiver performance is to average the SINR over N consecutive symbols, i.e.,

$$\begin{aligned} SINR_{av} &= E[SINR_i] \\ &= \sum_{i=1}^{N} P_r(SINR_i \mid J_i) P_r(J_i) \\ &= \frac{1}{N} \sum_{i=1}^{N} SINR_i \end{aligned} \tag{5}$$

where $SINR_i$ and $SINR_{av}$ denote, respectively, the receiver signal-to-interference-and-noise ratio over the i^{th} symbol and the average receiver SINR. In the above equation, $SINR_i$ is treated as a discrete random variable that takes N possible values with equal probability. $J_i (i = 1,\ldots,N)$ are the segments of the jammer signal over N consecutive symbols. In equation (5) $P_r(x)$ denotes the probability of the event x, and $P_r(J_i)=1/N$. The $SINR_i$ is

$$SINR_i = \frac{2P(Q - \sum_{k=0}^{Q-1} |\beta_{ik}|^2)}{\sigma^2}. \tag{6}$$

Accordingly,

$$SINR_{av} = \frac{2P(Q - \frac{1}{N} \sum_{i=1}^{N} \sum_{k=0}^{Q-1} |\beta_{ik}|^2)}{\sigma^2}. \tag{7}$$

The above expression, although simple to calculate, smoothes out high and low SINR values. In this regard, the average value in (7) does not properly penalize poor or reward good receiver performance. Further, it is difficult to establish a relationship between the receiver $SINR_{av}$ and its BER. Most importantly, expression (7) does not account for the self-noise term that reflects the level of signal distortion produced by the induced correlation of the code chips as a result of the excision process. Hence, a more proper way to measure the receiver performance is to deal with y_1 as a random variable. In this case the average receiver signal to interference plus noise ratio is referred to as $\overline{SINR}$ to distinguish it from equation (1). We assume that symbol "1" is transmitted and contaminated by one of N possible jammer signals occurring with the same probability. In this case, the mean value and the variance of the correlator output due to the GPS signal can be derived as

$$E[y_1] = \sum_{i=1}^{N} E[y_1 \mid J_i] P_r(J_i) = \frac{1}{N} \sum_{i=1}^{N} E[y_1 \mid J_i]$$
$$= \frac{\sum_{i=1}^{N} [P(Q - \sum_{k=0}^{Q-1} |\beta_{ik}|^2)]}{N} = PQ(1 - \frac{1}{NQ} \sum_{i=1}^{N} \sum_{k=0}^{Q-1} |\beta_{ik}|^2) \tag{8}$$

$$\sigma_{y_1}^2 = E[y_1^2] - E^2[y_1]$$
$$= \frac{1}{N} \sum_{i=1}^{N} P^2 (Q - \sum_{k=0}^{Q-1} |\beta_{ik}|^2)^2 - P^2 Q^2 (1 - \frac{1}{NQ} \sum_{i=1}^{N} \sum_{k=0}^{Q-1} |\beta_{ik}|^2)^2$$
$$= \frac{P^2}{N} \sum_{i=1}^{N} (\sum_{k=0}^{Q-1} |\beta_{ik}|^2)^2 - \frac{P^2}{N^2} (\sum_{i=1}^{N} \sum_{k=0}^{Q-1} |\beta_{ik}|^2)^2 \tag{9}$$

Similarly, the average noise power is

$$
\begin{aligned}
\sigma_{y_2}^2 &= E[y_2^2] = \sum_{i=1}^{N} E[y_2^2 \mid J_i] P_r(J_i) \\
&= \frac{1}{N} \sum_{i=1}^{N} E[y_2^2 \mid J_i] \\
&= \frac{\sum_{i=1}^{N} \sigma^2 P(Q - \sum_{k=0}^{Q-1} |\beta_{ik}|^2)}{N} \\
&= \sigma^2 PQ(1 - \frac{1}{NQ} \sum_{i=1}^{N} \sum_{k=0}^{Q-1} |\beta_{ik}|^2)
\end{aligned}
\tag{10}
$$

From the above and (1) the average SINR is given by,

$$
\begin{aligned}
\overline{SINR} &= \frac{E^2[y_1]}{\sigma_{y_1}^2 + \frac{1}{2}\sigma_{y_2}^2} \\
&= \frac{P^2 Q^2 (1 - \frac{1}{NQ} \sum_{i=1}^{N} \sum_{k=0}^{Q-1} |\beta_{ik}|^2)^2}{\frac{P}{N} \sum_{i=1}^{N} (\sum_{k=0}^{Q-1} |\beta_{ik}|^2)^2 - \frac{P}{N^2} (\sum_{i=1}^{N} \sum_{k=0}^{Q-1} |\beta_{ik}|^2)^2 + \frac{1}{2}\sigma^2 Q(1 - \frac{1}{NQ} \sum_{i=1}^{N} \sum_{k=0}^{Q-1} |\beta_{ik}|^2)}
\end{aligned}
\tag{11}
$$

This expression represents the SINR of the receiver implementing subspace projections to remove a periodic jammer and is also valid for the case in which the jammer assumes N possible waveforms. In the case that the jammer has the same period as the GPS data symbol, then N=1 and the above equation simplifies to single antenna case. Comparing (11) to (7) and SINR expression in Chapter 1, it is clear that (11) includes the self-noise component $\sigma_{y_1}^2$ that arises due to the differences in the distortion effects of interference excision on the GPS signal over the N symbols. In the absence of jamming, no excision is necessary, and the SINR of the receiver output becomes $2PQ/\sigma^2$, which represents the upper bound of the interference suppression performance. Moreover, if the jammer and the spreading codes are orthogonal, i.e., $\beta_{ik} = 0$, the interference suppression is also achieved with no loss in optimum receiver performance.

It is noted, however, that the values of the cross-correlation coefficient, $|\beta_{ik}|$, between the PN sequence signal and the non-stationary FM jammer are typically very small. This allows the proposed projection technique to excise FM jammers effectively with insignificant signal loss. Computer simulations show that $|\beta_{ik}|$ ranges from 0 to 0.14. With these values, the self-noise $\sigma_{y_1}^2$ is negligible compared to the Gaussian noise for the low SNR conditions that often prevail in GPS environment. In this case, equation (11) can be simplified to the following

$$\overline{SINR} \approx \frac{E^2[y_1]}{\frac{1}{2}\sigma_{y_2}^2} = \frac{2PQ\left(1-\frac{1}{NQ}\sum_{i=1}^{N}\sum_{k=0}^{Q-1}|\beta_k|^2\right)}{\sigma^2} \tag{12}$$

which is similar to the SINR expression in Chapter 1 and has the same form as (7). Therefore, $SINR_{av}$ and $\overline{SINR}$ approximately yield the same performance measure.

III. Simulation Results

Fig. 1 plots the receiver SINR vs SNR according to (11) for the two cases of N=1 and N/M=5/3. In both cases, the normalized start and end frequencies of the chirp jammer are 0 and 0.5, respectively. The SNR values range from –25dB to –5dB, and the GPS signal is the Gold code of satellite SV#1. It is clear that the period of the jammer has little effects on the result of interference suppression performance, as both SINR curves are very close to the upper bound. From Fig. 1, we can also observe that the SINR change linearly with the input SNR, which can be easily recognized from (12). Fig. 2 shows the $|\beta_{ik}|$ values for the underlying example. It is evident from this figure that there is no clear variation patterns of the cross-correlation coefficients. The range values of $|\beta_{ik}|$ do not

change greatly over different symbols. Experiments with different N, M, chirp rate, and satellite signals have given similar results.

IV. Conclusions

Subspace projection techniques were employed as a pre-correlation signal processing method in the GPS receiver to excise non-stationary FM jammers. Previous developments in receiver performance evaluation for periodic interferers have only considered the special case of jammers having the same period as the GPS symbol. This report establishes the derivation for the receiver SINR expression for non-stationary FM jammers with general periodic structures. It was argued that in the general case the FM jammer contaminates each GPS symbol with a finite number of possible waveforms. Two averaging measures to evaluate the overall SINR performance have been discussed and compared. The simulations included in this report employed chirp interferers and it was shown that these two measures give similar performance for this jammer class. The results suggest that the subspace projection method can excise periodic FM jammers effectively with insignificant losses to the desired signal.

References

[1] M. G. Amin and A. Akansu, "Time-frequency for interference excision in spread-spectrum communications," *Highlights of Signal Processing for Communications, Celebrating a Half Century of Signal Processing, editor: G. Giannakis*, IEEE Signal Processing Magazine, vol. 16 no.2, March 1999.

[2] M. G. Amin, "Interference mitigation in spread-spectrum communication systems using time-frequency distributions," *IEEE Trans. Signal Processing*, vol. 45, no. 1, pp. 90-102, Jan. 1997.

[3] C. Wang and M. G. Amin, "Performance analysis of instantaneous frequency based interference excision techniques in spread spectrum communications," *IEEE Trans. Signal Processing*, vol. 46, no. 1, pp. 70-83, Jan. 1998.

[4] S. Ramineni, M. G. Amin, and A. R. Lindsey, "Performance Analysis of Subspace Projection Techniques in DSSS Communications," Proceedings of the International Conference on Acoustics, Speech, and Signal Processing, Istanbul, Turkey, May 2000.

[5] L. Zhao, M. G. Amin, and A. R. Lindsey, "Subspace projection techniques for anti-FM jamming GPS receivers," *Proceedings of the 10-th IEEE Workshop on Statistical Signal and Array Processing*, pp. 529-533, Aug. 2000.

[6] L. Zhao, M. G. Amin, and A. R. Lindsey, "Subspace Array Processing for the Suppression of FM Jamming in GPS Receivers," Proceedings of the Asilomar Conference on Signals, Systems, and Computers, Monterey, CA, Oct. 2000.

[7] B. Boashash, "Estimating and interpreting the instantaneous frequency of a signal," Parts 1 and 2, *Proceedings of the IEEE*, vol. 80, no. 12, Dec. 1990.

[8] L. Cohen, *Time-Frequency Analysis*, Prentice Hall, Englewood Cliffs, New Jersey, 1995.

[9] B. W. Parkinson, J. J. Spilker Jr. eds, *Global Positioning System: Theory and Applications*, American Institute of Aeronautics and Astronautics, 1996.

[10] M. S. Braasch and A. J. Van Dierendonck, "GPS receiver architectures and measurements," *Proceedings of the IEEE*, Jan. 1999.

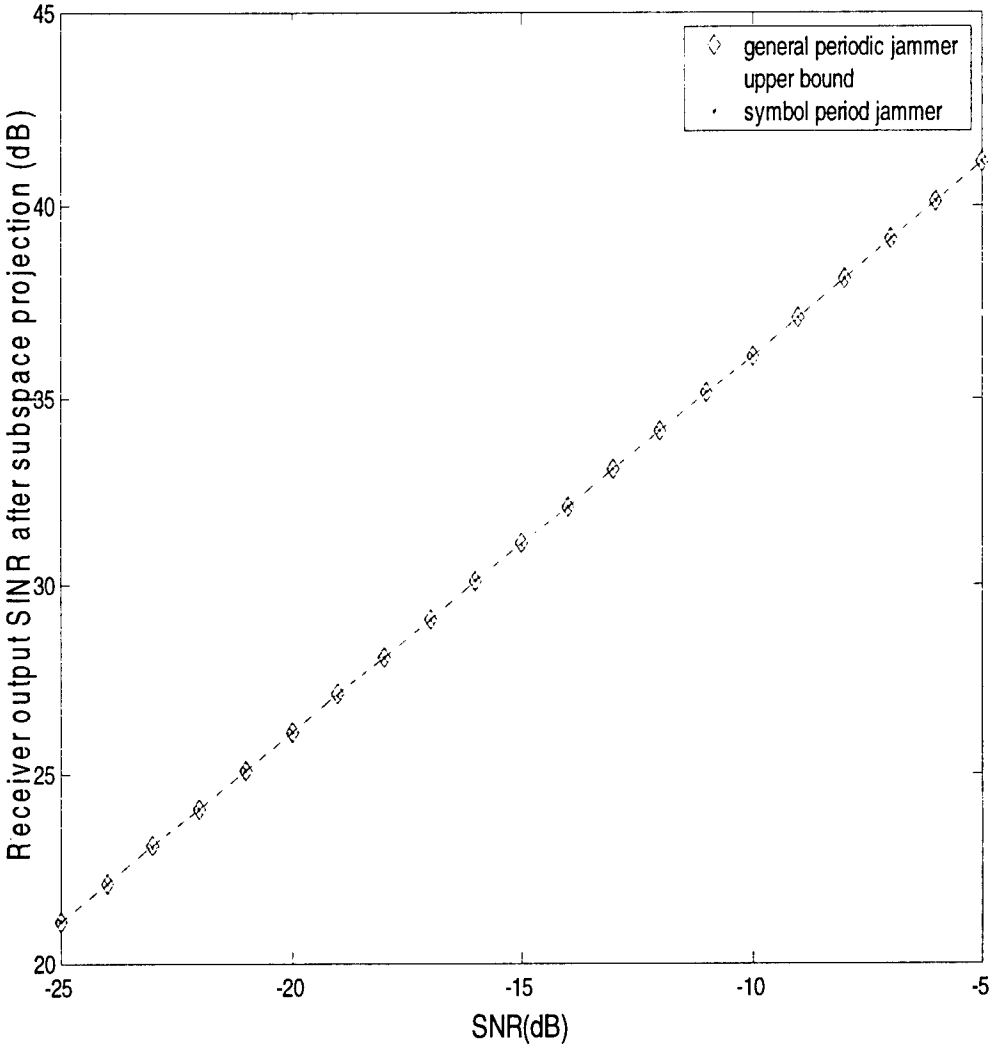

Figure 1. Output SINR vs SNR.

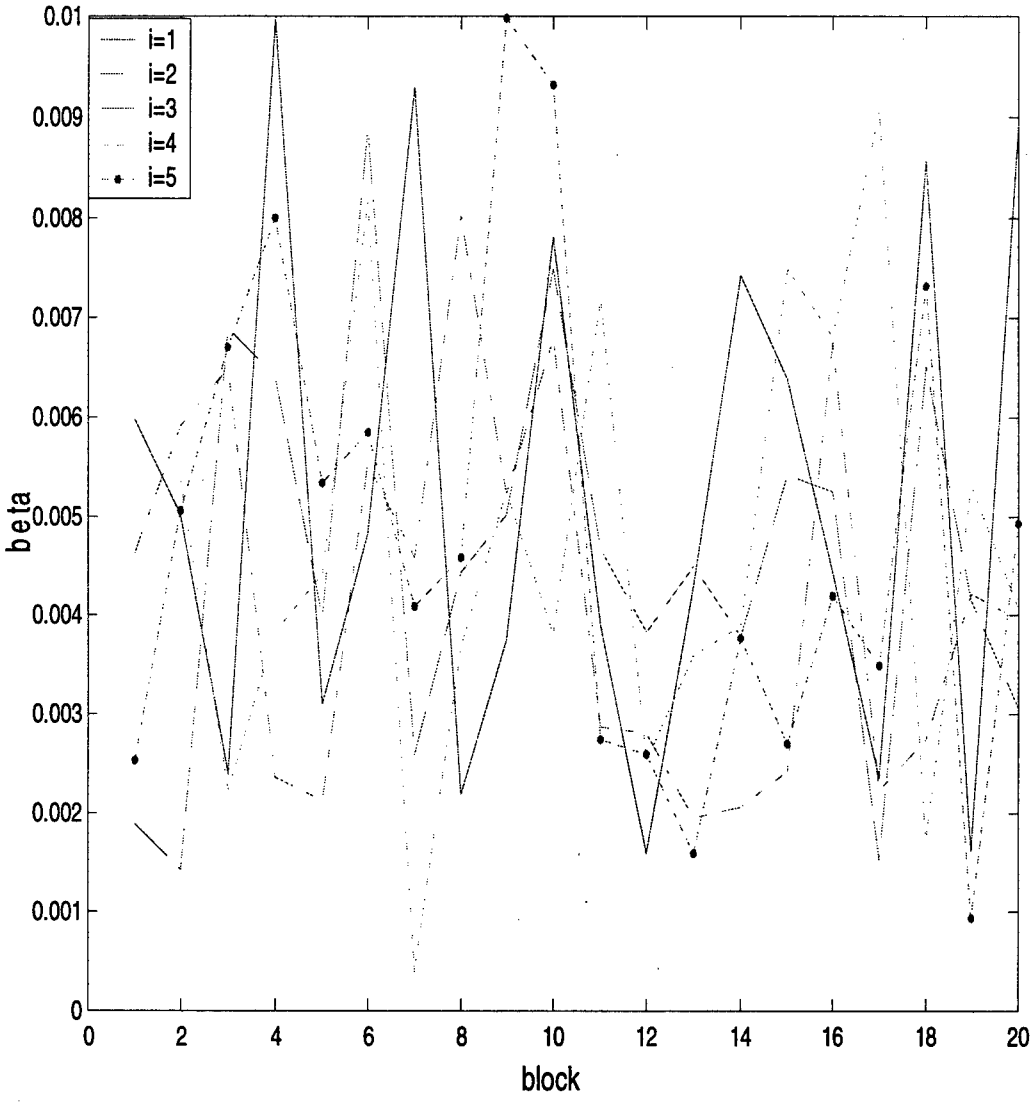

Figure 2. $|\beta_{ik}|$ for different symbols and blocks.

Chapter 3

Subspace Array Processing for the Suppression of FM Jammers in GPS Receivers

Abstract

This report applies the subspace projection array processing techniques for suppression of frequency modulated (FM) jammers in GPS receivers. The FM jammers are instantaneous narrowband and have clear time-frequency (t-f) signatures that are distinct from the GPS C/A spread spectrum code. In the proposed technique, the instantaneous frequency (IF) of the jammer is estimated and used to construct the jammer subspace. With a multi-sensor receiver, both spatial and time-frequency signatures of signal arrivals are used for effective interference suppression. This report considers the deterministic nature of the GPS C/A code. We derive the receiver SINR, which shows improved performance in strong interference environments.

I. Introduction

Compared with the subspace projection techniques in the single-sensor case, the use of multi-sensor array greatly increases the dimension of the available signal subspace. It allows both the distinctions in the spatial and temporal signatures of the GPS signals from those of the interferers to play equal roles in suppressing the jammer with a minimum distortion of the desired signal. In this report, we examine the applicability of multi-sensor subspace projection techniques for suppressing nonstationary jammers in GPS receivers.

We mainly address the problem of anti-jamming for the C/A code. This code has interesting properties due to the fact that it is periodic within one data symbol and fixed for each satellite signal. It is shown that this periodicity has a considerable effect on the receiver performance.

II. Subspace projection array processing

In GPS, the PN sequence of length L (1023) repeats itself Q (20) times within one symbol of the 50 bps navigation data. We use discrete-time form, where all the signals are sampled at the chip-rate of the C/A code. We consider an antenna array of N sensors, and the communication channel is restricted to flat-fading. In the proposed interference excision approach, the LNQ sensor output samples are partitioned into Q blocks, each of L chips and LN samples. The jammer can be consecutively removed from the 20 blocks that constitute on symbol. This is achieved by projecting the received data in each block on the corresponding orthogonal subspace of the jammer. The jammer-free signal is then correlated with the replica PN sequence on a symbol-by-symbol basis. We first consider

the subspace projection within each block. The array output vector at the k-th sample is given by

$$\begin{aligned} \boldsymbol{x}(k) &= \boldsymbol{x}_s(k) + \boldsymbol{x}_u(k) + \boldsymbol{b}(k) \\ &= c(k)\boldsymbol{h} + \sum_{i=1}^{U} A_i u_i(k)\boldsymbol{a}_i + \boldsymbol{b}(k) \end{aligned} \tag{1}$$

where $\mathbf{x}_s$, $\mathbf{x}_u$, and $\mathbf{b}$ are the signal, the jammer and the white Gaussian noise contributions, respectively. $\mathbf{h}$ is the signal spatial signature, and c(k) is the spreading PN sequence. The number of jammers is U. All jammers are considered as instantaneously narrowband FM signals with constant amplitude $u_i(k)=\exp[j\varphi_i(k)]$. A_i and $\mathbf{a}_i$ are the i-th jammer amplitude and the spatial signature, respectively. Furthermore, we normalize the channels and set $\|\mathbf{h}\|_F^2 = N$ and $\|\mathbf{a}\|_F^2 = N$, where $\|\cdot\|_F^2$ is the Frobenius norm of a vector. The noise vector $\mathbf{b}(k)$ is zero-mean, temporally and spatially white with

$$\begin{aligned} E[\boldsymbol{b}(k)\boldsymbol{b}^T(k+l)] &= 0 \\ E[E[\boldsymbol{b}(k)\boldsymbol{b}^H(k+l)] &= \sigma^2\delta(l)\boldsymbol{I}_N \end{aligned} \tag{2}$$

where σ^2 is the noise power, and I_N is the N×N identity matrix. Using L sequential array vector samples within the block, we obtain the following LN-by-1vector

$$\begin{aligned} \boldsymbol{X} &= [\boldsymbol{x}^T(1) \;\; \boldsymbol{x}^T(2) \;\; \ldots \;\; \boldsymbol{x}^T(L)]^T \\ &= \boldsymbol{X}_s + \boldsymbol{X}_u + \boldsymbol{B} \end{aligned} \tag{3}$$

The vector $\mathbf{X}_u$ consists of the U jammer signals, and is expressed as

$$\boldsymbol{X}_u = \sum_{i=1}^{U} A_i \boldsymbol{V}_i \tag{4}$$

with

$$\boldsymbol{V}_i = [u_i(1) \;\; u_i(2) \;\; \ldots \;\; u_i(L)]^T \otimes \boldsymbol{a}_i \tag{5}$$

where ⊗ denotes the Kronecker product. Therefore,

$$V = [V_1 \;\; V_2 \;\; \ldots \;\; V_U] \tag{6}$$

spans the jammer signal subspace, and its orthogonal subspace projection matrix is given by

$$P = I_{LN} - V(V^H V)^{-1} V^H = I_{LN} - \frac{1}{LN} VV^H \tag{7}$$

The projection of the received signal vector onto the orthogonal subspace yields

$$X_\perp = PX = PX_s + PB \tag{8}$$

which excises the jammers entirely. The signal vector $\mathbf{X}_s$ can be rewritten as

$$X_s = [c(1) \;\; c(2) \;\; \ldots \;\; c(L)]^T \otimes h \;\; \underline{\underline{\Delta}} \;\; q \tag{9}$$

where the vector **q** represents the spatial-temporal signature of the GPS signal. The result of despreading in the subspace projection based array system over one block is

$$y = q^H X_\perp = q^H Pq + q^H PB \;\; \underline{\underline{\Delta}} \;\; y_1 + y_2 \tag{10}$$

where y_1 and y_2 are the contributions of the PN and the noise sequences to the decision variable, respectively. For simplification, we assume that the jammers share the same period as the GPS data symbol. In GPS systems, due to the fact that each satellite is assigned a fixed Gold code [3], and that the Gold code is the same for every navigation data symbol, y_1 is a deterministic value, rather than a random variable as it is the case in many spread spectrum applications. The value of y_1 is given by

$$
\begin{aligned}
y_1 &= \boldsymbol{q}^H \boldsymbol{P} \boldsymbol{q} = \boldsymbol{q}^H (\boldsymbol{I}_{LN} - \frac{1}{LN} \boldsymbol{V} \boldsymbol{V}^H) \boldsymbol{q} \\
&= \boldsymbol{q}^H \boldsymbol{q} - \frac{1}{LN} \boldsymbol{q}^H \begin{bmatrix} \boldsymbol{V}_1 & \boldsymbol{V}_2 & \cdots & \boldsymbol{V}_U \end{bmatrix} \begin{bmatrix} \boldsymbol{V}_1 \\ \boldsymbol{V}_2 \\ \vdots \\ \boldsymbol{V}_U \end{bmatrix} \boldsymbol{q} \\
&= LN - \frac{1}{LN} \boldsymbol{q}^H \left(\sum_{i=1}^{U} \boldsymbol{V}_i \boldsymbol{V}_i^H \right) \boldsymbol{q} \\
&= LN - \frac{1}{LN} \sum_{i=1}^{U} \boldsymbol{q}^H \boldsymbol{V}_i \boldsymbol{V}_i^H \boldsymbol{q}
\end{aligned}
\tag{11}
$$

where

$$
\boldsymbol{q}^H \boldsymbol{V}_i = (\boldsymbol{c} \otimes \boldsymbol{h})^H (\boldsymbol{u}_i \otimes \boldsymbol{a}_i) = (\boldsymbol{c}^H \boldsymbol{u}_i)(\boldsymbol{h}^H \boldsymbol{a}_i) \tag{12}
$$

Define

$$
\alpha_i = \frac{\boldsymbol{h}^H \boldsymbol{a}_i}{N} \tag{13}
$$

as the spatial cross-correlation coefficient between the signal and the i-th jammer, and

$$
\beta_i = \frac{\boldsymbol{c}^T \boldsymbol{u}_i}{L} \tag{14}
$$

as the temporal cross-correlation coefficient between the PN sequence and the i-th jammer vector. Therefore,

$$
\boldsymbol{q}^H \boldsymbol{V}_i = LN \alpha_i \beta_i \tag{15}
$$

$$
y_1 = LN - LN \sum_{i=1}^{U} |\alpha_i|^2 |\beta_i|^2 = LN \left(1 - \sum_{i=1}^{U} |\alpha_i|^2 |\beta_i|^2 \right) \tag{16}
$$

From the above equation, it is clear that y_1 is real, which is due to the Hermitian property of the projection matrix **P**. With the assumptions in (2), y_2 is complex Gaussian with zero-mean. Therefore,

$$E[y] = y_1 = LN\left(1 - \sum_{i=1}^{U} |\alpha_i|^2 |\beta_i|^2\right) \tag{17}$$

$$\begin{aligned} Var[y] &= Var[y_2] = E[|y_2|^2] \\ &= E[\boldsymbol{q}^H \boldsymbol{P}\boldsymbol{B}\boldsymbol{B}^H \boldsymbol{P}^H \boldsymbol{q}] = \boldsymbol{q}^H \boldsymbol{P} E[\boldsymbol{B}\boldsymbol{B}^H] \boldsymbol{P}\boldsymbol{q} \\ &= \sigma^2 \boldsymbol{q}^H \boldsymbol{P}\boldsymbol{P}\boldsymbol{q} = \sigma^2 \boldsymbol{q}^H \boldsymbol{P}\boldsymbol{q} \\ &= \sigma^2 y_1 = \sigma^2 LN\left(1 - \sum_{i=1}^{U} |\alpha_i|^2 |\beta_i|^2\right) \end{aligned} \tag{18}$$

The above two equations are derived for only one block of the signal symbol. Below, we add subscript m to identify y with block m (m=1, 2, …, Q). By summing all Q blocks, we obtain the output of the symbol-level despreading,

$$y = \sum_{m=1}^{Q} y_m \tag{19}$$

Since y_m are Gaussian with zero-mean, y is also a zero-mean Gaussian random variable. The decision variable y_r is the real part of y,

$$y_r = \mathrm{Re}[y] \tag{20}$$

The expected value of y_r is

$$\begin{aligned} E[y_r] = E[y] &= \sum_{m=1}^{Q} y_m \\ &= LN\left(Q - \sum_{m=1}^{Q}\sum_{i=1}^{U} |\alpha_{mi}|^2 |\beta_{mi}|^2\right) \\ &= LN\left[Q - \sum_{i=1}^{U}\left(|\alpha_i|^2 \sum_{m=1}^{Q} |\beta_{mi}|^2\right)\right] \end{aligned} \tag{21}$$

where α_{mi} and β_{mi} are the spatial and temporal cross-correlation coefficients between the signal and the i-th jammer over block m. Since the changes in the spatial signatures of

the signals and jammers are very small compared with the period of one block (1 ms), α_{mi} can be simplified to α_i. The variance of y_r is

$$\begin{aligned}\sigma_{y_r}^2 &= \frac{1}{2}\sigma_y^2 = \frac{1}{2}\sum_{m=1}^{Q}\sigma_{y_m}^2 \\ &= \frac{1}{2}\sigma^2 LN\left[Q - \sum_{i=1}^{U}\left(|\alpha_i|^2 \sum_{m=1}^{Q}|\beta_{mi}|^2\right)\right]\end{aligned} \tag{22}$$

Therefore, the receiver SINR expression after projection and despreading is given by

$$\begin{aligned}SINR &= \frac{E^2[y]}{Var[y]} \\ &= \frac{2LN\left[Q - \sum_{i=1}^{U}\left(|\alpha_i|^2 \sum_{m=1}^{Q}|\beta_{mi}|^2\right)\right]}{\sigma^2}\end{aligned} \tag{23}$$

The temporal and spatial coefficients appear as multiplicative products in (23). This implies that the spatial and temporal signatures play equal roles in the receiver performance. In the absence of the jammers, no excision is necessary, and the SINR of the receiver output will become $2LNQ/\sigma^2$, which represents the upper bound of the interference suppression performance. Clearly, the term

$$2LN\sum_{i=1}^{U}\left(|\alpha_i|^2 \sum_{m=1}^{Q}|\beta_{mi}|^2\right) \tag{24}$$

in equation (23) is the reduction in the receiver performance caused by the proposed interference suppression technique. It reflects the energy of the signal component that is in the jammer subspace. It is important to note that if the jammers and the DSSS signal are orthogonal, either in spatial domain (α_i=0) or in temporal domain (β_{mi}=0), the interference excision is achieved with no loss in performance. In the general case, β_{mi} are very small and much smaller than α_i. Therefore, the difference in the temporal signatures

effectively with only insignificant signal loss. The spatial cross-correlation coefficients α_i are fractional values and, as such, further reduce the undesired term in (24).

Interference suppression using arrays is improved in several ways. First, the employment of an antenna array can lead to an accurate IF estimation of the jammers [9]. Second, in comparison with the result of the single sensor case [10],

$$SINR = \frac{2L\left(Q - \sum_{i=1}^{U}\sum_{m=1}^{Q}|\beta_{mi}|^2\right)}{\sigma^2} \tag{25}$$

multi-sensor receivers, at minimum, improve SINR by the array gain. This is true, independent of the underlying fading channels and scattering environment. As discussed above, compared to the temporal signatures, the contributions of spatial cross-correlation coefficients α_i in influencing the receiver SINR are, in most cases, insignificant.

III. Simulation Results

In this section, we present some simulation results illustrating the properties of the performance of the proposed projection technique. Fig. 1 depicts the SINR expression as a function of the input SNR. We consider two uncorrelated chirp jammers. The angle-of-arrival (AOA) of the satellite signal and the jammers are 5^0, 40^0, and 60^0, respectively. A two-element array is considered with half-wavelength spacing. The satellite PN sequence is the Gold code of satellite SV#1, and the normalized frequency of the jammers are from 0.01 to 0.2 and from 0.5 to 0.3, respectively. The SINR of the single sensor case is also plotted for comparison. The array gain is evident in Fig. 1. In this example, $|\alpha_1|$=0.643, $|\alpha_2|$=0.340, $|\beta_1|$ is in the range [0.0049-0.0604], and $|\beta_2|$ is in the range [0.0067-0.0839]. With the above values, the term (24) is far less than $2LNQ$, which allows SINR (23) to be very close to its upper bound.

IV. Conclusions

In this report, suppression of frequency modulation interferers in GPS using antenna arrays and subspace projection techniques is examined. It is shown that both the spatial and temporal signatures of the signals impinging on the multi-sensor receiver assume similar roles in the receiver performance. The spatial and temporal signatures' respective correlation coefficients appear as square multiplicative products in the SINR expression. However, due to the Gold code structure and the length of the PN, the differences in the temporal characteristics of the jammer and the C/A code yield negligible temporal correlation coefficients. These small values allow the receiver to perform very close to the no-jamming case, irrespective of the satellites and the jammers' angles of arrival. The array fundamental offering in the underlying interference suppression problem is through its gain, which is determined by the number of antennas employed at the receiver, as shown in Fig. 1.

References

[1] M. G. Amin and A. Akansu, "Time-frequency for interference excision in spread-spectrum communications," *Highlights of Signal Processing for Communications, Celebrating a Half Century of Signal Processing, editor: G. Giannakis*, IEEE SP Magazine, vol. 16 no.2, March 1999.

[2] M. G. Amin, "Interference mitigation in spread-spectrum communication systems using time-frequency distributions," *IEEE Trans. Signal Processing*, vol. 45, no. 1, pp. 90-102, Jan. 1997.

[3] C. Wang and M. G. Amin, "Performance analysis of instantaneous frequency based interference excision techniques in spread spectrum communications," *IEEE Trans. Signal Processing*, vol. 46, no. 1, pp. 70-83, Jan. 1998.

[4] M. Amin, C. Wang, and A. Lindsey, "Optimum interference excision in spread spectrum communications using open loop adaptive filters, " *IEEE Trans. Signal Processing*, vol. 47, no. 7, pp. 1966-1976, July 1999.

[5] Y. Zhang and M. G. Amin, "Blind beamforming for suppression of instantaneously narrowband signals in DS/SS communications using subspace projection techniques," *Proc. SPIE: Digital Wireless Communication II*, vol. 4045, Orlando, FL, April 2000.

[6] B. W. Parkinson, J. J. Spilker Jr. eds, *Global Positioning System: Theory and Applications*, American Institute of Aeronautics and Astronautics, 1996.

[7] M. S. Braasch and A. J. Van Dierendonck, "GPS receiver architectures and measurements," *Proceedings of the IEEE*, Jan. 1999.

[8] R. Jr. Landry, P. Mouyon and D. Lekaim, "Interference mitigation in spread spectrum systems by wavelet coefficients thresholding," *European Trans. on Telecommunications*, vol. 9, pp. 191-202, Mar.-Apr. 1998.

[9] W. Mu, M. G. Amin, and Y. Zhang, "Bilinear signal synthesis in array processing," submitted to to *IEEE Trans. Signal Processing.*

[10] L. Zhao, M. G. Amin, and A. R. Lindsey, "Subspace projection techniques for anti-FM jamming GPS receivers," *Proceedings of the 10-th IEEE Workshop on Statistical Signal and Array Processing*, pp. 529-533, Aug. 2000.

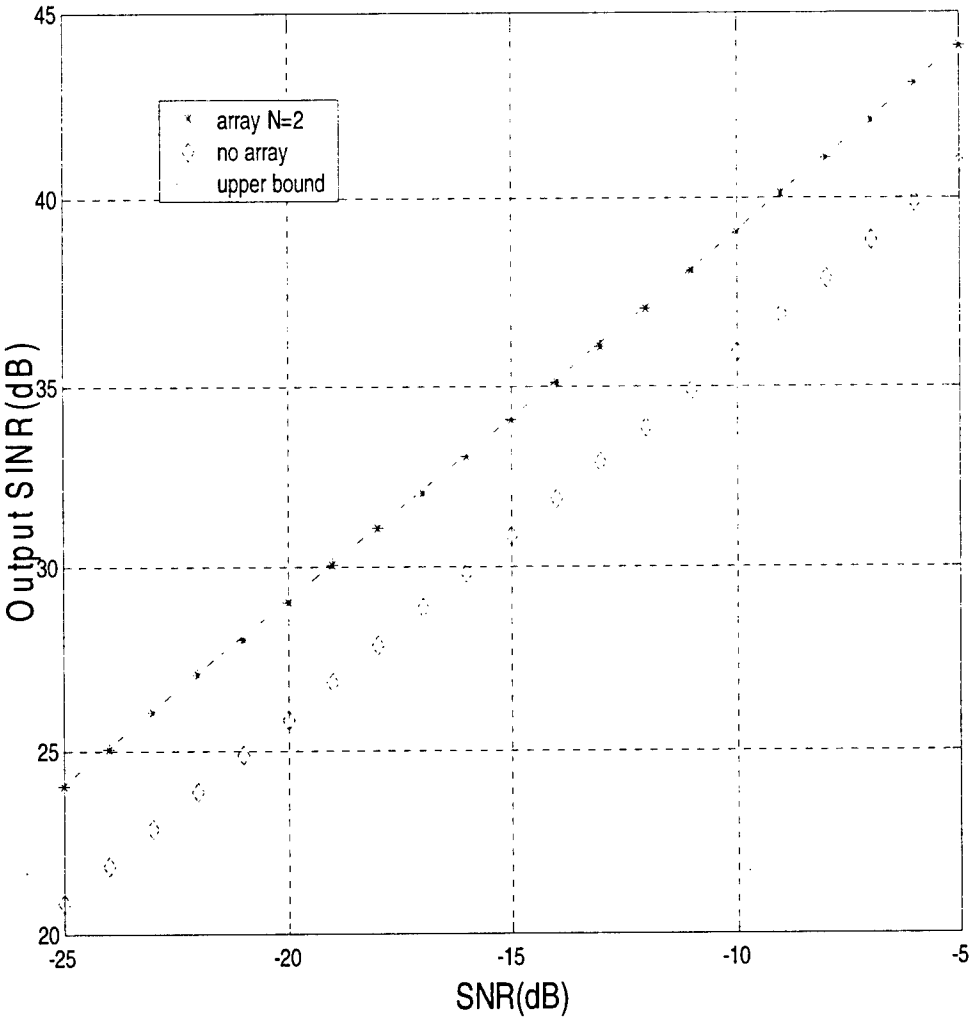

Fig. 1 Output SINR vs SNR

Chapter 4

Array Processing for Nonstationary Interference Suppression in DS/SS Communications Using Subspace Projection Techniques

Abstract

Combined spatial and time-frequency signatures of signal arrivals at a multi-sensor array are used for nonstationary interference suppression in direct-sequence spread-spectrum (DS/SS) communications. With random PN spreading code and deterministic nonstationary interferers, the use of antenna arrays offers increased DS/SS signal dimensionality relative to the interferers. Interference mitigation through spatio-temporal subspace projection technique leads to reduced DS/SS signal distortion and improved performance over the case of a single antenna receiver. The angular separation between the interference and desired signals is shown to play a fundamental role in trading off the contribution of the spatial and time-frequency signatures to the interference mitigation process. The expressions of the receiver SINR implementing subspace projections are derived and numerical results are provided.

I. Introduction

There are several methods that have been proposed for interference suppression in DS/SS communications, most have been related to one domain of operation [1], [2]. These methods include the narrowband interference waveform estimation [3], frequency domain interference excision [4], zero-forcing techniques [5], adaptive subspace-based techniques [6], [7], and minimum-mean-square error (MMSE) interference mitigation techniques [8].

Nonstationary interferers, which have model parameters that change with time, are particularly troublesome due to the inability of a single domain mitigation algorithm to adequately remove their effects. The recent development of the quadratic time-frequency distributions (TFDs) for improved signal power localization in the time-frequency plane has motivated several new approaches for excision of interference with rapidly time-varying frequency characteristics in the DS/SS communication systems. Comprehensive summary of TFD-based interference excision is given in reference [9]. The two basic methods for time-frequency excision are based on notch filtering and subspace projections. Utilization of the interference instantaneous frequency (IF), as obtained via TFDs, to design an open loop adaptive notch filter in the temporal domain, has been thoroughly discussed in [10], [11]. Subspace projection methods, commonly used for mitigating narrowband interference [12], [13], have been recently introduced for suppression of frequency modulated (FM) interference and shown to properly handle multi-component interference, reduce the self-noise, and improve the receiver performance beyond that offered by other time-frequency based techniques [14], [15], [16].

The main purpose of this chapter is to integrate spatial and temporal processing for suppression of nonstationary interferers in DS/SS systems. Specifically, we extend the projection-based interference mitigation techniques in [14], [15], [16] to multi-sensor array receivers. The proposed multi-sensor interference excision technique builds on the offerings of quadratic time-frequency distributions for estimation of 1) the time-frequency subspace

and time-frequency signature of nonstationary signals, and 2) the spatial signature of nonstationary sources using direction finding and blind source separations. With the knowledge of the time-frequency and spatial signatures, the objective is to effectively suppress strong nonstationary interferers with few array sensors. The proposed technique does not require the knowledge of the array response or channel estimation of the DS/SS signal, but it utilizes the distinction in both of its spatial- and time-frequency signatures from those of the interferers that impinge on the array. With the combined spatial-time-frequency signatures, the projection of the data vector onto the subspace orthogonal to that of the interferers leads to improved receiver performance over that obtained using the subspace projection in the single-sensor case.

The rest of the chapter is organized as follows. In Section II, the signal model is described. Section III briefly reviews the subspace projection technique. We present in Section IV blind beamforming based on subspace projection and derive the receiver output signal-to-interference-plus-noise ratio (SINR). Several numerical results are given in Section V. Section VI concludes this chapter.

II. Signal Model

In DS/SS communications, each symbol is spread into $L = T/T_c$ chips, where T and T_c are, respectively, the symbol duration and chip duration. We use discrete-time form, where all signal arrivals are sampled at the chip-rate of the DS/SS signal. The symbol-rate source signal is denoted as $s(n)$, and the aperiodic binary spreading sequence of the nth symbol period is represented by $c(n,l) \in \pm 1, l = 0, 1, \cdots, L-1$. The chip-rate sequence of the DS/SS signal can be expressed as

$$d(k) = s(n)c(n,l) \qquad \text{with} \quad k = nL + l. \tag{1}$$

For notation simplicity, we use $c(l)$ instead of $c(n,l)$ for the spreading sequence.

We consider an antenna array of N sensors. The propagation delay between antenna

elements is assumed to be small relative to the inverse of the transmission bandwidth, so that the received signal at the N sensors are identical to within complex constants. The received signal vector of the DS/SS signal at the array is expressed by the product of the chip-rate sequence $d(k)$ and its spatial signature $\underline{\mathrm{h}}$,

$$\underline{\mathrm{x}}_s(k) = d(k)\underline{\mathrm{h}}. \tag{2}$$

The channel is restricted to flat-fading, and is assumed fixed over the symbol length, and as such $\underline{\mathrm{h}}$ in the above equation is not a function of k.

The array vector associated with a total of U interference signals is given by

$$\underline{\mathrm{x}}_u(k) = \sum_{i=1}^{U} \underline{\mathrm{a}}_i u_i(k) \tag{3}$$

where $\underline{\mathrm{a}}_i$ is the array response to the ith interferer, $u_i(k)$. Without loss of generality, we set $||\underline{\mathrm{h}}||_F^2 = N$ and $||\underline{\mathrm{a}}_i||_F^2 = N$, $i = 1, 2, \cdots, U$, where $||\cdot||_F$ is the Frobenius norm of a vector. The input data vector is the sum of three components,

$$\underline{\mathrm{x}}(k) = \underline{\mathrm{x}}_s(k) + \underline{\mathrm{x}}_u(k) + \underline{\mathrm{b}}(k) = d(k)\underline{\mathrm{h}} + \sum_{i=1}^{U} \underline{\mathrm{a}}_i u_i(k) + \underline{\mathrm{b}}(k) \tag{4}$$

where $\underline{\mathrm{b}}(k)$ is the additive noise vector. In regards to the above equation, we make the following assumptions.

A1) The information symbols $s(n)$ is a wide-sense stationary process with $E[s(n)s^*(n)] = 1$, where the superscript * denotes complex conjugation. The spreading sequence $c(k)$ is a binary random sequence with $E[c(k)c(k+l)] = \delta(l)$, where $\delta(l)$ is the delta function.[1]

A2) The noise vector $\underline{\mathrm{b}}(k)$ is zero-mean, temporally and spatially white with

$$E[\underline{\mathrm{b}}(k)\underline{\mathrm{b}}^T(k+l)] = \mathbf{0} \quad \text{for all } l,$$

and

$$E[\underline{\mathrm{b}}(k)\underline{\mathrm{b}}^H(k+l)] = \sigma\delta(l)\mathbf{I}_N,$$

[1]This assumption is most suitable for military applications and P-code GPS.

where σ is the noise power, the superscripts ^{T} and ^{H} denote transpose and conjugate transpose, respectively, and $\mathbf{I}_N$ is the $N \times N$ identity matrix.

A3) The signal and noise are statistically uncorrelated.

III. Subspace Projection

The aim of subspace projection techniques is to remove the interference components before despreading by projecting the input data on the subspace orthogonal to the interference subspace, as illustrated in Fig. 1. The receiver block diagram is shown in Fig. 2.

A nonstationary interference, such as an FM signal, often shares the same bandwidth with the DS/SS signal and noise. As such, for a chirp signal or a signal with high-order frequency laws, the signal spectrum may span the entire frequency band, and the sample data matrix loses its complex exponential structure responsible for its singularity. Therefore, the interference subspace can no longer be obtained from the eigendecomposition of the sample data matrix [12], [14] or the data covariance matrix [13], as it is typically the case in stationary environments. The nonstationary interference subspace, however, may be constructed using the interference time-frequency signature. Methods for estimating the instantaneous frequency, instantaneous bandwidth, and more generally, a time-frequency subspace, based on the signal time-frequency localization properties are, respectively, discussed in references [17], [18], [14].

For the general class of FM signals, and providing that interference suppression is performed separately over the different data symbols, the interference subspace is one-dimensional in an L-dimensional space. We note that since an FM interference has a constant amplitude, its respective data vector can be determined from the IF up to a complex multiplication factor. The unit norm normalization of this vector represents the one-dimensional interference subspace basis vector. Among candidate methods of IF estimation is the one based on the time-frequency distributions. For example, the discrete

form of Cohen's class of TFD of a signal $x(t)$ is given by [19]

$$D_{xx}(t,f) = \sum_{m=-\infty}^{\infty} \sum_{\tau=-\infty}^{\infty} \phi(m,\tau) x(t+m+\tau) x^*(t+m-\tau) e^{-j4\pi f\tau}. \tag{5}$$

where $\phi(m,\tau)$ is a time-frequency kernel that could be signal-dependent. The TFD concentrates the interference signal power around the IF and makes it visible in the noise and PN sequence background [17], [20]. It has been shown that, for linear FM signals, Radon-Wigner transform provides improved IF estimates over the TFD [21]. Parametric methods using autoregressive model have also been proposed [22].

Other nonstationary interference with instantaneous bandwidth or spread in the time-frequency domain are captured in a higher-dimension subspace. In this case, the interference subspace can be constructed from the interference localization region Ω in the time-frequency domain (see, for example, [14]). The subspace of interest becomes that which fills out the interference time-frequency region Ω energetically, but has little or no energy outside Ω.

Interference-free DS/SS signals are obtained by projecting the received data vector (in the temporal domain processing, the vector consists of data samples at different snapshots) on the subspace orthogonal to the interference subspace.

A. Temporal Processing

In the single-sensor receiver, the input data is expressed as

$$x(k) = x_s(k) + x_u(k) + b(k) = d(k) + \sum_{i=1}^{U} u_i(k) + b(k). \tag{6}$$

Using L sequential chip-rate samples of one symbol of the received signals at time index k, we obtain the following input vector

$$\begin{aligned} &[x(k) \;\; x(k-1) \;\; \cdots \;\; x(k-L+1)]^T \\ &= [x_s(k) \;\; x_s(k-1) \;\; \cdots \;\; x_s(k-L+1)]^T \\ &+ [x_u(k) \;\; x_u(k-1) \;\; \cdots \;\; x_u(k-L+1)]^T \\ &+ [b(k) \;\; b(k-1) \;\; \cdots \;\; b(k-L+1)]^T \end{aligned} \tag{7}$$

or simply

$$X(k) = X_s(k) + X_u(k) + B(k). \tag{8}$$

We drop the variable k for simplicity, with the understanding that processing is performed over the nth symbol that starts at the kth chip. Then, equation (8) becomes

$$X = X_s + X_u + B. \tag{9}$$

Below, we relax the FM condition used in [12], [15] that translates to a single dimension interference. The general case of an interference occupying higher dimension subspace is considered. We assume that the ith interferer spans M_i dimensional subspace, defined by the orthonormal basis vectors, $V_{i,1}, V_{i,2}, \cdots, V_{i,M_i}$, and the different interference subspaces are disjoint. Define

$$V_i = [V_{i,1}\ V_{i,2}\ \cdots\ V_{i,M_i}] \tag{10}$$

and let $M = \sum_{i=1}^{U} M_i$ as the number of total dimensions of the interferers. With $L > M$, the $L \times M$ matrix

$$V = [V_1\ V_2\ \cdots\ V_U], \quad V_i \bigcap V_j = \Phi \quad \text{for } i \neq j \tag{11}$$

is full rank and its columns span the combined interference subspace J. The respective projection matrix is

$$\overline{P} = V\left(V^H V\right)^{-1} V^H. \tag{12}$$

The projection matrix associated with the interference orthogonal subspace, G, is then given by

$$P = \mathbf{I}_L - V(V^H V)^{-1} V^H. \tag{13}$$

When applied to X, matrix P projects the input data vector onto G, and results in

$$X_\perp = PX = PX_s + PB, \tag{14}$$

which no longer includes any interference component.

The single-sensor receiver implementing subspace projection for excision of a single instantaneously narrowband FM interferer (i.e., $U = 1, M_1 = 1$) in DS/SS communications is derived in [23]. The receiver SINR is shown to be

$$\text{SINR} = \frac{(L-1)^2}{\left(1-\frac{2}{L}\right)+\sigma(L-1)} = \frac{L-1}{\frac{L-2}{L(L-1)}+\sigma}. \tag{15}$$

For typical values of L, $(L-2)/(L-1) \approx 1$, and equation (15) can be simplified as

$$\text{SINR} \approx \frac{L-1}{\sigma+1/L}. \tag{16}$$

Compared to the interference-free environment, where the receiver SINR is L/σ, nonstationary interference suppression in (16) is achieved by reducing the processing gain by 1 and increasing the noise power by the self-noise factor of $1/L$.

IV. Subspace Projection in Multi-Sensor Receiver

In this section, we consider nonstationary interference excision in multi-sensor receivers using subspace projections. We note that if the subspace projection method discussed in Section III is extended to an N-element array by suppressing the interference independently in each sensor data and then combining the results by maximum ratio combining (see Fig. 3), then it is straightforward to show that the receiver SINR is given by

$$\text{SINR} \approx \frac{N(L-1)}{\sigma+N/L} \tag{17}$$

The above extension, although clearly improves over (16), does not utilize the potential difference in the spatial signatures of signal arrivals, and, therefore, is inferior to the receiver proposed in this Section.

A. Spatio-Temporal Signal Subspace Estimation

To construct the spatio-temporal signal subspace of the interference signals, it is important to estimate both the time-frequency signature (or subspace) and the spatial signature

of each interferer. The IF estimation of an FM interference signal based on time-frequency distribution is addressed in Section III. It is noteworthy that when multiple antennas are available, the TFD may be computed at each sensor data separately and then averaged over the array. This method has been shown in [24] to improve the IF estimation, as it reduces noise and crossterms that often obscure the source true power localization in the time-frequency domain.

On the other hand, the estimation of source spatial signature can be achieved, for example, by using direction finding and source separation techniques. When the interference signals have clear bearings, methods like MUSIC [25] and maximum likelihood (ML) [26] can be used to estimate the steering matrix of the interference signals. These methods can be revised to incorporate the TFD of the signal arrivals for improved performance [27], [28]. On the other hand, in fading channels where the steering vector loses its known structure due to multipath, blind source separation methods should be used [29], [30], [31]. Since the interferers in DS/SS communications often have relatively high power, good spatial signature estimation is expected.

More conveniently, the spatial signatures can be simply estimated by using matched filtering once the time-frequency signatures are provided. The maximum likelihood estimator for the vector $\underline{a}_i$ is obtained as

$$\hat{\underline{a}}_i = \sqrt{N} \sum_{k=0}^{L-1} \hat{u}_i^*(k)\underline{x}(k) / || \sum_{k=0}^{L-1} \hat{u}_i^*(k)\underline{x}(k) ||_F, \tag{18}$$

where $\hat{u}_i(k)$ is the estimated waveform of the ith interferer. It is noted that the possible phase ambiguity in the waveform estimation of $\hat{u}_i(k)$ does not affect the estimation of the spatial signature. For slowly varying channels, the above average can also be performed over multiple symbols to improve the estimation accuracy.

In the analysis presented herein, we assume knowledge of the interference subspace and its angle-of-arrival (AOA) to derive the receiver SINR.

B. Proposed Technique

The subspace projection problem for nonstationary interference suppression in DS/SS communications is now considered within the context of multi-sensor array using N array elements. We use one symbol DS/SS signal duration (i.e., L chip-rate temporal snapshots), and stack L discrete observations to construct an $NL \times 1$ vector of the received signal sequence in the joint spatio-temporal domain. In this case, the received signal vector in (4) becomes

$$\begin{aligned}
&\left[\underline{\mathrm{x}}^T(k) \;\; \underline{\mathrm{x}}^T(k-1) \;\; \cdots \;\; \underline{\mathrm{x}}^T(k-L+1)\right]^T \\
&= \left[\underline{\mathrm{x}}_s^T(k) \;\; \underline{\mathrm{x}}_s^T(k-1) \;\; \cdots \;\; \underline{\mathrm{x}}_s^T(k-L+1)\right]^T \\
&+ \left[\underline{\mathrm{x}}_u^T(k) \;\; \underline{\mathrm{x}}_u^T(k-1) \;\; \cdots \;\; \underline{\mathrm{x}}_u^T(k-L+1)\right]^T \\
&+ \left[\underline{\mathrm{b}}^T(k) \;\; \underline{\mathrm{b}}^T(k-1) \;\; \cdots \;\; \underline{\mathrm{b}}^T(k-L+1)\right]^T
\end{aligned} \tag{19}$$

or simply

$$\mathbf{X} = \mathbf{X}_s + \mathbf{X}_u + \mathbf{B}, \tag{20}$$

where again the variable k is dropped for simplicity.

In (19), the interference vector in the single-sensor problem, given by (7), is extended to a higher dimension. With the inclusion of both temporal and spatial samples, the mth basis of the ith interference becomes

$$\mathbf{V}_{i,m} = V_{i,m} \otimes \underline{\mathrm{a}}_i \tag{21}$$

and

$$\mathbf{V}_i = \left[\mathbf{V}_{i,1} \; \mathbf{V}_{i,2} \; \cdots \; \mathbf{V}_{i,M_i}\right], \tag{22}$$

where $\otimes$ denotes the Kronecker product. The columns of the $LN \times M$ matrix

$$\mathbf{V} = \left[\mathbf{V}_1 \; \mathbf{V}_2 \; \cdots \; \mathbf{V}_U\right] \tag{23}$$

spans the overall interference signal subspace.

For independent spatial signatures, the matrix rank is M. The orthogonal projection matrix is given by

$$\mathbf{P} = \mathbf{I}_{LN} - \mathbf{V}\left(\mathbf{V}^H\mathbf{V}\right)^{-1}\mathbf{V}^H. \tag{24}$$

The projection of the signal vector on the orthogonal subspace of the interferers' yields

$$\mathbf{X}_{\perp} = \mathbf{P}\mathbf{X} = \mathbf{P}\mathbf{X}_s + \mathbf{P}\mathbf{B}. \tag{25}$$

The block diagram of the proposed method is presented in Fig. 4. As shown in the next section, effective interference suppression can be achieved solely based on the spatial signatures or the time-frequency signatures, or it may require both information.

C. Performance Analysis

Below we consider the performance of the multi-sensor receiver system implementing subspace projections. Recall that

$$V_{i,m}^H V_{j,n} = 0 \quad \text{for any} \quad i, m \neq j, n. \tag{26}$$

and

$$\mathbf{V}^H\mathbf{V} = N\mathbf{I}_M, \tag{27}$$

the projection matrix $\mathbf{P}$ becomes

$$\mathbf{P} = \mathbf{I}_{LN} - \frac{1}{N}\mathbf{V}\mathbf{V}^H. \tag{28}$$

The signal vector $\mathbf{X}_s$ can be rewritten as

$$\begin{aligned} \mathbf{X}_s &= \left[\underline{\mathrm{x}}_s^T(k) \;\; \underline{\mathrm{x}}_s^T(k-1) \;\; \cdots \;\; \underline{\mathrm{x}}_s^T(k-L+1)\right]^T \\ &= \left[d(k)\underline{\mathrm{h}}^T \;\; d(k-1)\underline{\mathrm{h}}^T \;\; \cdots \;\; d(k-L+1)\underline{\mathrm{h}}^T\right]^T \\ &= s(n)\left[c(L-1)\; c(L-2) \;\; \cdots \;\; c(0)\right]^T \otimes \underline{\mathrm{h}} \\ &\underline{\underline{\triangle}}\; s(n)\mathbf{q}, \end{aligned} \tag{29}$$

where the $LN \times 1$ vector

$$\mathbf{q} = \left[c(L-1)\; c(L-2) \;\; \cdots \;\; c(0)\right]^T \otimes \underline{\mathrm{h}} \;\underline{\underline{\triangle}}\; \underline{\mathrm{c}} \otimes \underline{\mathrm{h}} \tag{30}$$

defines the spatio-temporal signature of the desired DS/SS signal. $\mathbf{q}$ is the extension of the DS/SS code by replicating it with weights defined by the signal spatial signature.

By performing despreading and beamforming, the symbol-rate decision variable is given by

$$y(n) = \mathbf{q}^H \mathbf{X}_\perp(k) = s(n)\mathbf{q}^H \mathbf{P}\mathbf{q} + \mathbf{q}^H \mathbf{P}\mathbf{B}(k) \triangleq y_1(n) + y_2(n), \tag{31}$$

where $y_1(n)$ is the contribution of the desired DS/SS signal to the decision variable, and $y_2(n)$ is the respective contribution from the noise.

The SINR of the array output becomes (see Appendix A)

$$\text{SINR} = \frac{E^2[y(k)]}{var[y(k)]} = \frac{\left(L - \sum_{i=1}^{U} M_i|\beta_i|^2\right)^2}{\left(\left(\sum_{i=1}^{U} M_i|\beta_i|^2\right)^2 - 2\sum_{i=1}^{U} \xi_i|\beta_i|^4\right) + \frac{\sigma}{N}\left(L - \sum_{i=1}^{U} M_i|\beta_i|^2\right)}, \tag{32}$$

where ξ_i is defined in (A.9), and β_i is the spatial correlation coefficient between the spatial signatures $\underline{\mathrm{h}}$ and $\underline{\mathrm{a}}_i, i = 1, 2, \cdots, U$, and is given by

$$\beta_i = \frac{1}{N}\underline{\mathrm{h}}^H \underline{\mathrm{a}}_i. \tag{33}$$

Note that when the noise power is small, i.e., $\sigma \ll 1$, the variance of y_1 becomes dominant, and the output SINR reaches the following upper bound

$$\text{SINR}_{\text{high SNR}} \approx \frac{\left(L - \sum_{i=1}^{U} M_i|\beta_i|^2\right)^2}{\left(\sum_{i=1}^{U} M_i|\beta_i|^2\right)^2 - 2\sum_{i=1}^{U} \xi_i|\beta_i|^4}. \tag{34}$$

This result is affected by the factors L, M_i, $|\beta_i|$, and $\xi_i, i = 1, \cdots, U$. On the other hand, when the noise level is very high, i.e., $\sigma \gg 1$, the noise variance plays a key role in determining $var[y(k)]$, and the output SINR becomes

$$\text{SINR}_{\text{low SNR}} \approx \frac{\left(L - \sum_{i=1}^{U} M_i|\beta_i|^2\right)^2}{\frac{\sigma}{N}\left(L - \sum_{i=1}^{U} M_i|\beta_i|^2\right)} = \frac{N}{\sigma}\left(L - \sum_{i=1}^{U} M_i|\beta_i|^2\right). \tag{35}$$

Unlike the high input SNR case, the output SINR in (35) also depends on both N and σ. Comparing (34) and (35), it is clear that the improvement in the receiver SINR becomes more significant when the spatial signatures produce small spatial correlation coefficients and under high SNR.

Next, we consider some specific important cases. When $\beta_i = 0, i = 1, \cdots, U$, $var[y_1(n)] = 0$, the receiver SINR in (32) becomes SINR $= LN/\sigma$. This is to say, the output SINR is improved by a factor of LN over the input signal-to-noise ratio (SNR) (not the input SINR!). This implies that the interferers are suppressed by spatial selectivity of the array and their suppression does not cause any distortion of the temporal characteristics of the DS/SS signal. The DS/SS signal in this case enjoys the array gain that contributes the factor N to the SINR.

For a single FM interferer ($U = 1$, $M_1 = 1$), equation (32) becomes

$$\text{SINR} = \frac{\left(L - |\beta_1|^2\right)^2}{\left(1 - \frac{2}{L}\right)|\beta_1|^4 + \frac{\sigma}{N}\left(L - |\beta_1|^2\right)}. \tag{36}$$

It is easy to show that SINR in (36) monotonously decreases as $|\beta_1|$ increases, and the lower bound of the SINR is reached for $\beta_1 = 1$, which is the case of the desired DS/SS signal and the interference signal arriving from the same direction. With a unit value of β_1,

$$\text{SINR} = \frac{(L-1)^2}{\left(1 - \frac{2}{L}\right) + \frac{\sigma}{N}(L-1)} \approx \frac{N(L-1)}{\frac{N}{L} + \sigma}. \tag{37}$$

This result is the same as that of the single-sensor case developed in [15], except for the appearance of the array gain, N, for the desired DS/SS signal over the noise. This equation also coincides with (17). That is, the independent multi-sensor subspace projection, illustrated in Fig. 3, results in the same output SINR with the proposed multi-sensor subspace projection method when $|\beta_1| = 0$.

On the other hand, the maximum value in (36) corresponds to $\beta = 0$, and is equal to SINR $= LN/\sigma$, as discussed above. For the illustration of the SINR behaviour, we plot

in Fig. 5 the SINR in (36) versus $|\beta_1|$ for a two-sensor array, where $L = 64$, and one FM jammer is considered with $M = 7$. The input SNR is 0dB.

Given the temporal and spatial signatures, the proposed technique simplifies to two consecutive tasks. The first is to estimate the spatio-temporal signature. When using multiple antenna receivers, a basis vector of the orthogonal projection matrix is obtained by the Kronecker product of a jammer's temporal signature and its spatial signature, that results in the $LN \times LN$ orthogonal project matrix instead of $L \times L$ in the single antenna case. The second task is jammer suppression via subspace projection. This involves the multiplication of an $LN \times LN$ matrix and an $LN \times 1$ vector.

Note such increase in computations is natural due to increase of dimensionality. It is noteworthy that array processing expands overall space dimensionality but maintains the jammer subspace dimension. As a result, it yields improved SINR performance over temporal processing or spatial processing only methods.

V. Numerical Results

A two-element array is considered with half-wavelength spacing. The DS/SS signal uses random spreading sequence with $L = 64$. The AOA of the DS/SS signal is 0 degree from broadside ($\theta_D = 0°$).

We consider two interference signals. Each interference signal is assumed to be made up of uncorrelated FM component with $M_i = 7, i = 1, 2$. The overall interference subspace is M=14. The AOAs of the two interferers are $\theta_J = [40°, 60°]$. The respective spatial correlations in this example are $|\beta_1| = 0.53$ and $|\beta_2| = 0.21$. Note that, in the subspace projection method, the output SINR is independent of the input jammer-to-signal ratio (JSR), since the interferers are entirely suppressed, regardless of their power. Fig. 6 shows the receiver SINR versus the input SNR. The upper bounds correspond to interference-free data. For high input SNR, the receiver SINR is decided by the induced signal distortion, described by the variance given in (A.10). It is evident from Fig. 6 that the two-antenna

receiver outperforms the single-antenna receiver case by a factor much larger than the array gain. Since the output SINR in the two-antenna receiver highly depends on the spatial correlation coefficients, the curves corresponding to a two-sensor array in Fig. 6 will assume different values upon changing β_1, or/and β_2. The best performance is achieved at $\beta_1 = \beta_2 = 0$.

Fig. 7 shows the receiver SINR versus the number of chips per symbol (L). We let L vary from 8 to 4096, whereas the input SNR is fixed at 0 dB. The two interference signals are incident on the array with angles $\theta_J = [40°, 60°]$. They are assumed to maintain their time-frequency spread with increased value of L. As such, the respective dimentions of their subspaces grow propotional to the number of chips per symbol. In this example, the dimension of each interference signal is assumed to be 10 percent of L (round to the nearest integer). The ouput SINR improvement by performing array processing at different L is evident from this figure. It is seen that, unlike the case of the instantaneously narrowband FM interference, where the output SINR increases rapidly as L increases, the output SINR in the underlying scenario ceases to increase as L assumes large values. This is because the rank of the interference signal subspace increases with L.

In Fig. 8 we investigate the receiver SINR performance versus the number of array sensors. In this figure, L is set at 64, and the input SNR is 0 dB. Two interference signals composed of uncorrelated FM components are considered, and $M_i = 7, i = 1, 2$, are assumed. Two examples are used to examine the effect of different AOAs. In the first example, $\theta_J = [40°, 60°]$. The output SINR improves sharply as the number of array sensors increases from one to three, beyond which the improvement becomes insignificant. The differences in the above AOAs of the desired DS/SS signal and the interference signals are relatively large, and a small number of array sensors leads to negligible spatial correlation coefficients. We also show a case with closely spaced interference signals where $\theta_J = [5°, 15°]$. In this case, the output SINR slowly improves as the number of array sensors increases.

It is noted that, when we consider a specific case, the output SINR does not increase monotonously with the number of array sensors. This is because the relationship between the spatial correlation coefficient and the AOAs is by itself not monotonous. Nevertheless, when we consider the general case with different AOA combinations, high number of array sensors often reduce the spatial correlation coefficients.

VI. Conclusions

In this chapter, subspace projection techniques were employed to suppress nonstationary interferers in direct sequence spread spectrum (DS/SS) communication systems. Interference suppression is based on the knowledge of both the interference time-frequency and spatial signatures. While the former is based on instantaneous frequency information that can be gained using several methods, including time-frequency distributions, the later can be provided from applying higher resolution methods or blind source separation techniques to the signal arrivals.

The differences between the DS/SS signal and interference signatures both in the time-frequency and spatial domains equip the projection techniques with the ability to remove the interference with a minimum distortion of the desired signal.

The receiver performance based on subspace projections was analyzed. It was shown that the lower performance bound is obtained when the sources have the same angular position. In this case, the problem becomes equivalent to a single-antenna receiver with only the presence of the array gain. On the other hand, the upper bound on performance is reached in the interference-free environment and also corresponds to the case in which the spatial signature of the interference is orthogonal to that of the DS/SS signal.

Numerical results were presented to illustrate the receiver SINR dependency on spatial correlation coefficient, input SNR, and the PN sequence length.

Appendix A

To derive the output SINR expression, we use $s(n) = +1$ (the output SINR is independent of $s(n)$ and same result follows when $s(n) = -1$). Then,

$$\begin{aligned} E[y_1(n)] &= E\left[\mathbf{q}^H\mathbf{P}\mathbf{q}\right] \\ &= E\left[\mathbf{q}^H(\mathbf{I} - \frac{1}{N}\mathbf{V}\mathbf{V}^H)\mathbf{q}\right] \\ &= E\left[\mathbf{q}^H\mathbf{q}\right] - \frac{1}{N}E\left[\mathbf{q}^H\mathbf{V}\mathbf{V}^H\mathbf{q}\right] \\ &= LN - \frac{1}{N}E\left[\mathbf{q}^H\sum_{i_1=1}^{U}\mathbf{V}_{i_1}\sum_{i_2=1}^{U}\mathbf{V}_{i_2}^H\mathbf{q}\right] \\ &= LN - \frac{1}{N}E\left[\mathbf{q}^H\sum_{i_1=1}^{U}\sum_{m_1=1}^{M_i}\mathbf{V}_{i_1,m_1}\sum_{i_2=1}^{U}\sum_{m_2=1}^{M_i}\mathbf{V}_{i_2,m_2}^H\mathbf{q}\right]. \end{aligned} \tag{A.1}$$

It is straightforward to show that

$$\mathbf{q}^H\mathbf{V}_{i,m} = (\underline{c}\otimes\underline{h})^H(V_{i,m}\otimes\underline{a}_i) = \left(\underline{c}^T V_{i,m}\right)\otimes\left(\underline{h}^H\underline{a}_i\right) = N\beta_i\sum_{l=0}^{L-1}V_{i,m}(l)c(l). \tag{A.2}$$

Using the orthogonal property of the spreading sequence A1), (A.1) becomes

$$\begin{aligned} E[y_1(n)] &= LN - NE\left[\sum_{i_1=1}^{U}\beta_{i_1}\sum_{m_1=1}^{M_{i_1}}\sum_{l_1=0}^{L-1}V_{i_1,m_1}(l_1)c(l_1)\sum_{i_2=1}^{U}\beta_{i_2}^*\sum_{m_2=1}^{M_{i_2}}\sum_{l_2=0}^{L-1}V_{i_2,m_2}^*(l_2)c(l_2)\right] \\ &= LN - N\sum_{i=1}^{U}|\beta_i|^2\sum_{m=1}^{M_i}\sum_{l=0}^{L-1}|V_{i,m}(l)|^2c^2(l) \\ &= N\left(L - \sum_{i=1}^{U}M_i|\beta_i|^2\right). \end{aligned} \tag{A.3}$$

Due to the zero-mean property of noise (assumption A2), $E[y_2(n)] = 0$. Accordingly,

$$E[y(n)] = E[y_1(n)] = N\left(L - \sum_{i=1}^{U}M_i|\beta_i|^2\right). \tag{A.4}$$

It is clear from (A.4) that the increase in the space dimensionality from L to NL does not simply translate into a corresponding increase in the desired mean value, or subsequently in the processing gain. Also, from assumption A3), the cross-correlation between $y_1(n)$ and $y_2(n)$ is zero, i.e.,

$$E[y_1^*(n)y_2(n)] = E[y_1(n)y_2^*(n)] = 0. \tag{A.5}$$

Therefore, the mean square value of the decision variable is made up of only two terms.

$$E\left[|y(n)|^2\right] = E\left[|y_1(n)|^2\right] + E\left[|y_2(n)|^2\right]. \tag{A.6}$$

The first term is the mean square value of $y_1(n)$. From (26), we have

$$E\left[|y_1(n)|^2\right] = E\left[\mathbf{q}^H\mathbf{P}\mathbf{q}\mathbf{q}^H\mathbf{P}^H\mathbf{q}\right]$$

$$= E\left[\mathbf{q}^H\left(\mathbf{I}_N - \frac{1}{N}\mathbf{V}\mathbf{V}^H\right)\mathbf{q}\mathbf{q}^H\left(\mathbf{I}_{LN} - \frac{1}{LN}\mathbf{V}\mathbf{V}^H\right)\mathbf{q}\right]$$

$$= E\left[\mathbf{q}^H\mathbf{q}\mathbf{q}^H\mathbf{q}\right] - \frac{2}{N}E\left[\mathbf{q}^H\mathbf{q}\mathbf{q}^H\mathbf{V}\mathbf{V}^H\mathbf{q}\right] + \frac{1}{N^2}E\left[\mathbf{q}^H\mathbf{V}\mathbf{V}^H\mathbf{q}\mathbf{q}^H\mathbf{V}\mathbf{V}^H\mathbf{q}\right]$$

$$= (LN)^2 - 2LN^2\sum_{i=1}^{U} M_i|\beta_i|^2$$

$$+N^2E\left[\sum_{i_1=1}^{U}\beta_{i_1}\sum_{m_1=1}^{M_{i_1}}\sum_{l_1=0}^{L-1}V_{i_1,m_1}(l_1)c(l_1)\sum_{i_2=1}^{U}\beta_{i_2}^*\sum_{m_2=1}^{M_{i_2}}\sum_{l_2=0}^{L-1}V_{i_2,m_2}^*(l_2)c(l_2)\right.$$
$$\left.\times\sum_{i_3=1}^{U}\beta_{i_3}\sum_{m_3=1}^{M_{i_3}}\sum_{l_3=0}^{L-1}V_{i_3,m_3}(l_3)c(l_3)\sum_{i_4=1}^{U}\beta_{i_4}^*\sum_{m_4=1}^{M_{i_4}}\sum_{l_4=0}^{L-1}V_{i_4,m_4}^*(l_4)c(l_4)\right]$$

$$= (LN)^2 - 2LN^2\sum_{i=1}^{U} M_i|\beta_i|^2$$

$$+N^2E\left[\sum_{i_1=i_2=1}^{U}\beta_{i_1}\beta_{i_2}^*\sum_{m_1=m_2=1}^{M_{i_1}}\sum_{l_1=l_2=0}^{L-1}V_{i_1,m_1}(l_1)V_{i_2,m_2}^*(l_2)c(l_1)c(l_2)\right.$$
$$\left.\times\sum_{i_3=i_4=1}^{U}\beta_{i_3}\beta_{i_4}^*\sum_{m_3=m_4=1}^{M_{i_3}}\sum_{l_3=l_4=0}^{L-1}V_{i_3,m_3}(l_3)V_{i_4,m_4}^*(l_4)c(l_3)c(l_4)\right]$$

$$+N^2E\left[\sum_{i_1=i_4=1}^{U}\beta_{i_1}\beta_{i_4}^*\sum_{m_1=m_4=1}^{M_{i_1}}\sum_{l_1=l_4=0}^{L-1}V_{i_1,m_1}(l_1)V_{i_4,m_4}^*(l_4)c(l_1)c(l_4)\right.$$
$$\left.\times\sum_{i_3=i_2=1}^{U}\beta_{i_3}\beta_{i_2}^*\sum_{m_3=m_2=1}^{M_{i_3}}\sum_{l_3=l_2=0}^{L-1}V_{i_3,m_3}(l_3)V_{i_2,m_2}^*(l_2)c(l_3)c(l_2)\right]$$

$$+N^2E\left[\sum_{i_1=i_3=1}^{U}\beta_{i_1}\beta_{i_3}\sum_{m_1=1}^{M_{i_1}}\sum_{m_3=1}^{M_{i_3}}\sum_{l_1=l_3=0}^{L-1}V_{i_1,m_1}(l_1)V_{i_3,m_3}(l_3)c(l_1)c(l_3)\right.$$
$$\left.\times\sum_{i_2=i_4=1}^{U}\beta_{i_2}^*\beta_{i_4}^*\sum_{m_2=1}^{M_{i_2}}\sum_{m_4=1}^{M_{i_4}}\sum_{l_2=l_4=0}^{L-1}V_{i_2,m_2}^*(l_2)V_{i_4,m_4}^*(l_4)c(l_2)c(l_4)\right]$$

$$-2N^2E\left[\sum_{i_1=i_2=i_3=i_4=1}^{U}\beta_{i_1}\beta_{i_2}^*\beta_{i_3}\beta_{i_4}^*\sum_{m_1=m_2=m_3=m_4=1}^{M_{i_1}}\right.$$
$$\left.\times\sum_{l_1=l_2=l_3=l_4=0}^{L-1}V_{i_1,m_1}(l_1)V_{i_2,m_2}^*(l_2)V_{i_3,m_3}(l_3)V_{i_4,m_4}^*(l_4)c(l_1)c(l_2)c(l_3)c(l_4)\right]$$

$$= (LN)^2 - 2LN^2 \sum_{i=1}^{U} M_i|\beta_i|^2 + N^2 \left(2 \left(\sum_{i=1}^{U} M_i|\beta_i|^2 \right)^2 + \left| \sum_{i=1}^{U} \beta_i^2 \gamma_i \right|^2 - 2 \sum_{i=1}^{U} \xi_i |\beta_i|^4 \right), \quad \text{(A.7)}$$

where

$$\gamma_i = \sum_{m_1=1}^{M_i} \sum_{m_2=1}^{M_i} \sum_{l=1}^{L-1} V_{i,m_1}(l) V_{i,m_2}(l) \quad \text{(A.8)}$$

and

$$\xi_i = \sum_{m=1}^{M_i} \sum_{l=1}^{L-1} |V_{i,m}(l)|^4 . \quad \text{(A.9)}$$

In practice, γ_i takes negligible values, and equation (A.7) can be simplified to

$$E\left[|y_1(n)|^2\right] = (LN)^2 - 2LN^2 \sum_{i=1}^{U} M_i|\beta_i|^2 + N^2 \left(2 \left(\sum_{i=1}^{U} M_i|\beta_i|^2 \right)^2 - 2 \sum_{i=1}^{U} \xi_i |\beta_i|^4 \right). \quad \text{(A.10)}$$

The value of ξ_i depends on the type of interference signals. Specifically, when the ith interference signal is made up of a single FM or a number of uncorrelated FM signal components, then the basis vectors are of constant modulus, and

$$\xi_i = \frac{M_i}{L}. \quad \text{(A.11)}$$

The second term of (A.6) is the mean-square value of $y_2(n)$,

$$\begin{aligned} E\left[|y_2(n)|^2\right] &= E\left[\mathbf{q}^H \mathbf{P}\mathbf{B}(k)\mathbf{B}^H(k)\mathbf{P}^H\mathbf{q}\right] \\ &= \sigma E\left[\mathbf{q}^H \mathbf{P}\mathbf{P}^H\mathbf{q}\right] = \sigma E\left[\mathbf{q}^H \mathbf{P}\mathbf{q}\right] = \sigma N \left(L - \sum_{i=1}^{U} M_i|\beta_i|^2 \right). \end{aligned} \quad \text{(A.12)}$$

The variance of $y(n)$ is given by

$$\begin{aligned} var[y(n)] &= E[|y(n)|^2] - E^2[y(n)] \\ &= E[|y_1(n)|^2] + E[|y_2(n)|^2] - E^2[y_1(n)] \\ &= (LN)^2 - 2LN^2 \sum_{i=1}^{U} M_i|\beta_i|^2 + N^2 \left(2 \left(\sum_{i=1}^{U} M_i|\beta_i|^2 \right)^2 - \frac{1}{L} \sum_{i=1}^{U} M_i|\beta_i|^4 \right) \\ &\quad + \sigma N \left(L - \sum_{i=1}^{U} M_i|\beta_i|^2 \right) - N^2 \left(L - \sum_{i=1}^{U} M_i|\beta_i|^2 \right)^2 \\ &= N^2 \left(\left(\sum_{i=1}^{U} M_i|\beta_i|^2 \right)^2 - 2 \sum_{i=1}^{U} \xi_i |\beta_i|^4 \right) + \sigma N \left(L - \sum_{i=1}^{U} M_i|\beta_i|^2 \right). \end{aligned} \quad \text{(A.13)}$$

Equation (32) follows by using the results of (A.4) and (A.13).

References

[1] H. V. Poor and L. A. Rusch, "Narrowband interference suppression in spread-spectrum CDMA," *IEEE Personal Comm. Mag.*, vol. 1, no. 8, pp. 14–27, Aug. 1994.

[2] J. D. Laster and J. H. Reed, "Interference rejection in digital wireless communications," *IEEE Signal Processing Mag.*, vol. 14, no. 3, pp. 37–62, May 1997.

[3] J. Wang and L. B. Milstein, "Adaptive LMS filters for cellular CDMA overlay," *IEEE J. Select. Areas Commun.*, vol. 14, no. 8, pp. 1548–1559, Oct. 1996.

[4] S. Sandberg, "Adapted demodulation for spread-spectrum receivers which employ transform-domain interference excision," *IEEE Trans. Commun.*, vol. 43, pp. 2502–2510, Sept. 1995.

[5] L. A. Rusch and H. Poor, "Multiuser detection techniques for narrow-band interference suppression in spread spectrum communications," *IEEE Trans. Commun.*, vol. 43, no. 2/3/4, pp. 1725–1737, Feb./Mar./Apr. 1995.

[6] H. Fathallah and L. A. Rusch, "A subspace approach to adaptive narrow-band interference suppression in DSSS," *IEEE Trans. Commun.*, vol. 45, no. 12, pp. 1575–1585, Dec. 1997.

[7] M. Lops, G. Ricci, and A. T. Tulino, "Narrow-band-interference suppression in multiuser CDMA systems," *IEEE Trans. Signal Processing*, vol. 46, no. 9, pp. 1163–1175, Sept. 1998.

[8] L. A. Rusch, "MMSE detector for narrow-band interference suppression in DS spread spectrum," in *Proc. Interference Rejection and Signal Separation in Wireless Commun. Symp.*, Newark, NJ, March 1996.

[9] M. G. Amin and A. Akansu, "Time-frequency for interference excision in spread-spectrum communications," in "Highlights of signal processing for communications: celebrating a half century of signal processing," *IEEE Signal Processing Mag.*, vol. 16, no. 2, March 1999.

[10] M. G. Amin, "Interference mitigation in spread spectrum communication systems using time-frequency distribution," *IEEE Trans. Signal Processing*, vol. 45, no. 1, pp.90–102, Jan. 1997.

[11] M. G. Amin, C. Wang, and A. Lindsey, "Optimum interference excision in spread spectrum communications using open loop adaptive filters," *IEEE Trans. Signal Processing*, vol. 47, no. 7, pp.1966–1976, July 1999.

[12] B. K. Poh, T. S. Quek, C. M. S. See, and A. C. Kot, "Suppression of strong narrowband interference using eigen-structure-based algorithm," in *Proc. Milcom*, pp. 1205–1208, July 1995.

[13] A. Haimovich and A. Vadhri, "Rejection of narrowband interferences in PN spread spectrum systems using an eigenanalysis approach," in *Proc. IEEE Signal Processing Workshop on Statistical Signal and Array Processing*, Quebec, Canada, pp. 1002–1006, June 1994.

[14] F. Hlawatsch and W. Kozek, "Time-frequency projection filters and time-frequency signal expansions," *IEEE Trans. Signal Processing*, vol. 42, no. 12, pp. 3321–3334, Dec. 1994.

[15] M. G. Amin and G. R. Mandapati, "Nonstationary interference excision in spread spectrum communications using projection filtering methods," in *Proc. 32nd Annual Asilomar Conf. on Signals, Systems, and Computers*, Pacific Grove, CA, Nov. 1998.

[16] S. Barbarossa and A. Scaglione, "Adaptive time-varying cancellation of wideband interferences in spread-spectrum communications based on time-frequency distributions," *IEEE Trans. Signal Processing*, vol. 47, no. 4, pp. 957–965, April 1999.

[17] B. Boashash, "Estimating and interpreting the instantaneous frequency of a signal," *Proc. IEEE*, vol. 80, no. 12, Dec. 1990.

[18] P. Loughlin and K. Davidson, "Instantaneous bandwidth of multicomponent signals," in *Proc. SPIE: Advanced Signal Processing Algorithms, Architectures, and Implementations IX*, vol. 3807, pp. 546–551, July 1999.

[19] L. Cohen, *Time-Frequency Analysis*, Prentice Hall, 1995.

[20] P. Rao and F. J. Taylor, "Estimation of the instantaneous frequency using the discrete Wigner distribution," *Electronics Lett.*, vol. 26, no. 4, pp. 246–248, Feb. 1990.

[21] M. Wang, A. Chan, and C. Chui, "Linear frequency-modulated signal detection using Radon-ambiguity transform," *IEEE Trans. Signal Processing*, vol. 46, no. 3, pp. 571–586, March 1998.

[22] P. Shan abd A. A. Beex, "FM interference suppression in spread spectrum communications using time-varying autoregressive model based instantaneous frequency estimation," in *Proc. IEEE Int. Conf. on Acoustics, Speech, and Signal Processing*, Phoenix, AZ, pp. 2559–2562, March 1999.

[23] R. S. Ramineni, M. G. Amin, and A. R. Lindsey, "Performance analysis of subspace projection techniques for interference excision in DSSS communications," in *Proc. IEEE Int. Conf. on Acoustics, Speech, and Signal Processing*, Istanbul, Turkey, June 2000.

[24] W. Mu, Y. Zhang, and M. G. Amin, "Bilinear signal synthesis in array processing," in *Proc. IEEE Int. Conf. on Acoustics, Speech, and Signal Processing*, Salt Lake City, UT, May 2001.

[25] R. O. Schmidt, "Multiple emitter location and signal parameter estimation," *IEEE Trans. Antennas Propagat.*, vol. 34, no. 3, pp. 276–280, March 1986.

[26] I. Ziskind and M. Wax, "Maximum likelihood localization of multiple sources by alternating projection," *IEEE Trans. Acoust., Speech, Signal Processing*, vol. ASSP-36, no. 10, pp. 1553–1560, Oct. 1988.

[27] A. Belouchrani and M. Amin, "Time-frequency MUSIC," *IEEE Signal Processing Lett.*, vol. 6, no. 5, pp. 109–110, May 1999.

[28] Y. Zhang, W. Mu, and M. G. Amin, "Time-frequency maximum likelihood methods for direction finding," *J. Franklin Inst.*, vol. 337, no. 4, pp. 483–497, July 2000.

[29] J. F. Cardoso, A. Belouchrani, K. Abed Maraim, and E. Moulines, "A blind source separation technique using second order statistics," *IEEE Trans. Signal Processing*,

vol. 45, no. 2, pp. 434–444, Feb. 1997.

[30] A. Belouchrani and M. Amin, "Blind source separation based on time-frequency signal representation," *IEEE Trans. Signal Processing*, vol. 46, no. 11, pp. 2888–2898, Nov. 1998.

[31] Y. Zhang and M. G. Amin, "Blind separation of sources based on their time-frequency signatures," in *Proc. IEEE Int. Conf. on Acoustics, Speech, and Signal Processing*, Istanbul, Turkey, June 2000.

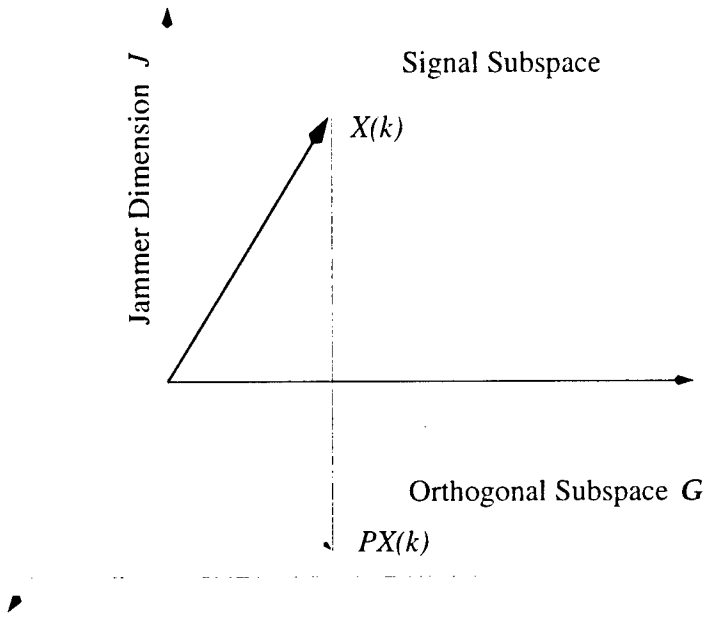

Fig. 1 Jammer suppression by subspace projection.

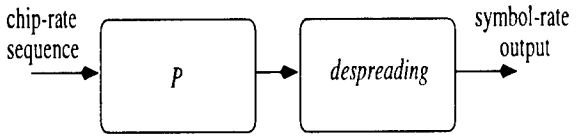

Fig. 2 Block diagram of single-sensor subspace projection.

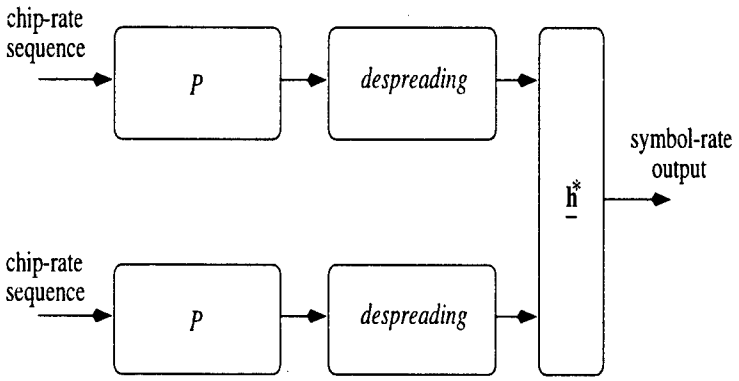

Fig. 3 Block diagram of independent multi-sensor subspace projection.

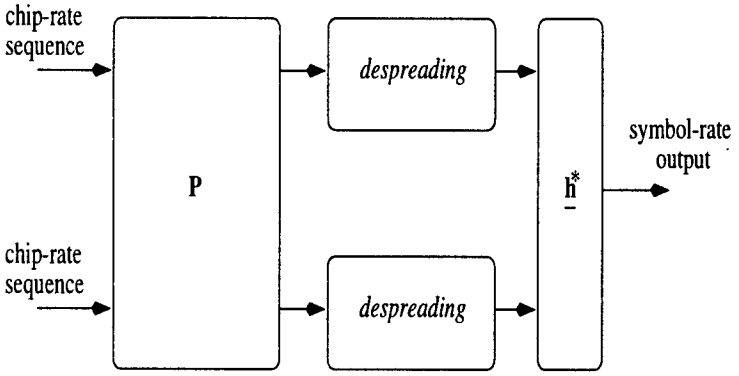

Fig. 4 Block diagram of proposed multi-sensor subspace projection.

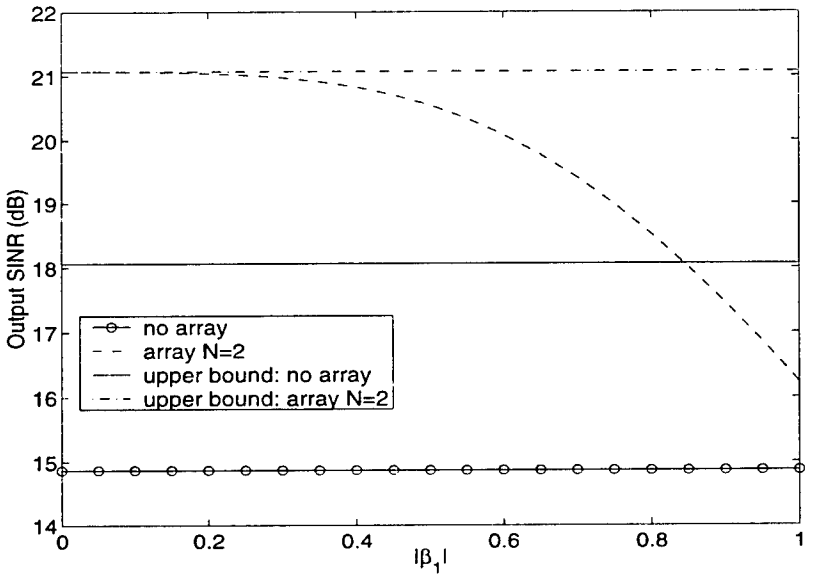

Fig. 5 Output SINR versus $|\beta_1|$ (input SNR=0dB, L=64, U=1, M=7).

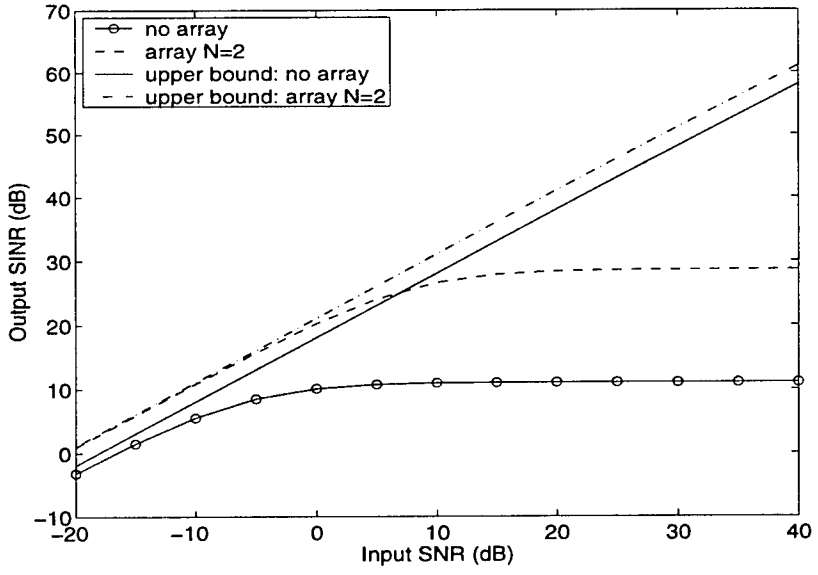

Fig. 6 Output SINR versus input SNR
(L=64, U=2, $M_1 = M_2 = 7$, $\theta_D = 0°$, $\theta_J = [40°, 60°]$).

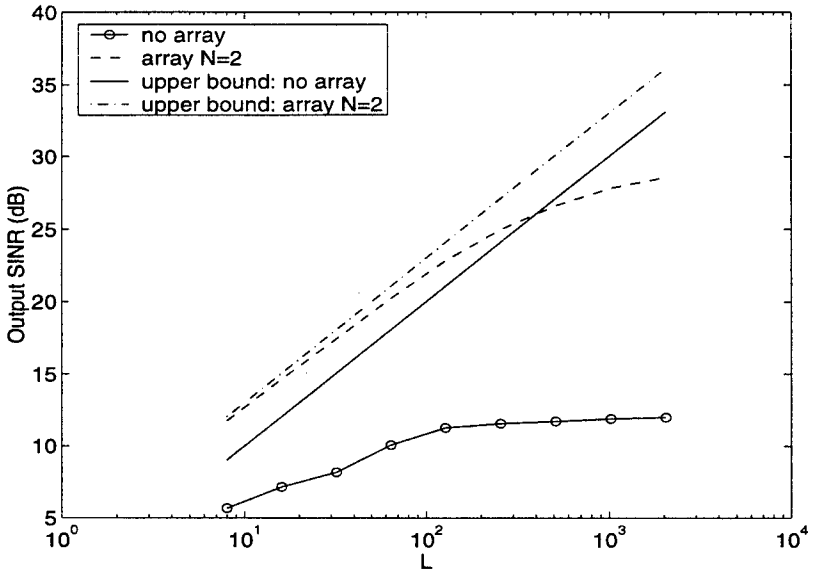

Fig. 7 Output SINR versus the number of chips per symbol (L) (input SNR=0dB, U=2, $M_1 = M_2 = 7$, $\theta_D = 0°$, $\theta_J = [40°, 60°]$).

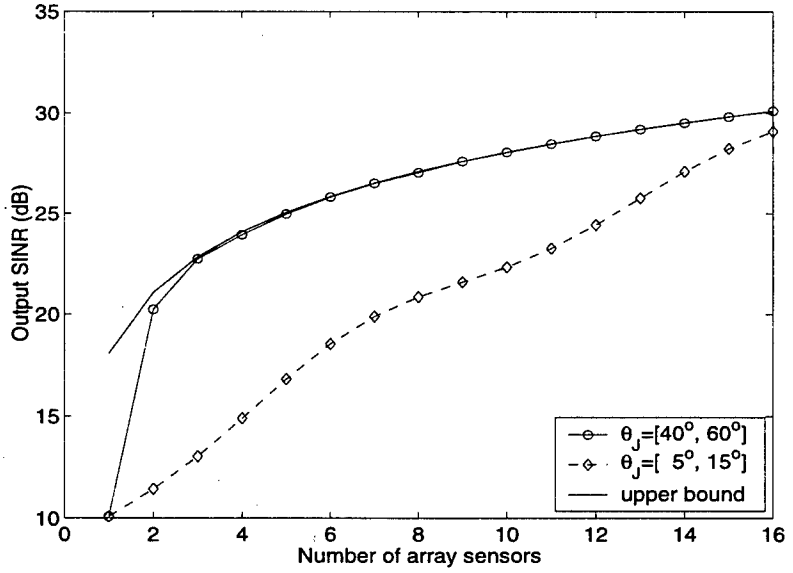

Fig. 8 Output SINR versus the number of array sensors (input SNR=0dB, L=64, U=2, $M_1 = M_2 = 7$).

☆U.S. GOVERNMENT PRINTING OFFICE: 2001-710-038-10179

MISSION
OF
AFRL/INFORMATION DIRECTORATE (IF)

The advancement and application of Information Systems Science and Technology to meet Air Force unique requirements for Information Dominance and its transition to aerospace systems to meet Air Force needs.